Energy Reports 16 (2026) 109610

Contents lists available at ScienceDirect

Energy Reports

journal homepage: www.elsevier.com/locate/egyr

Research paper

Data-driven decarbonisation strategies for ships, part 1: Technical feasibility and emissions modelling

Li Chin Law [a,e,*], Nikolaos Tsoulakos [c], Evita Meristoudi [d], Panos Theodossopoulos [d], Epaminondas Mastorakos [a,b,*]

[a] Cambridge Centre for Advanced Research and Education in Singapore (CARES), CREATE Tower, 1 Create Way, 138602, Singapore
[b] Engineering Department, University of Cambridge, Cambridge CB2 1PZ, UK
[c] Laskaridis Shipping Co. Ltd, Athens, Greece
[d] Metis Cyberspace Technology, Attica, Kallithea, Greece
[e] EMICAST, CREATE Tower, 1 Create Way, 138602, Singapore

ARTICLE INFO

Keywords:
Feasibility study
Conceptual design
Carbon capture
Low carbon alternative fuel
Maritime
Ship decarbonization

ABSTRACT

This paper investigates the feasibility of retrofitting a 10-year-old bulk carrier into a low-emissions ship without compromising vessel performance, using a data-driven ship design approach. Two years of high-frequency operational data were analysed to support the conceptual design of alternative fuel systems and carbon capture pathways, with techno-economic assessments based on realistic CAPEX and OPEX estimates. An optimal fuel containment capacity of 50 million MJ was selected for alternative fuels including LNG, hydrogen, ammonia, methanol, biodiesel, and electricity. For the fossil fuels, different on-board carbon capture and storage (CCS) configurations were compared, revealing a wide range of capture rates (19.7–82.8%) and fuel penalties (9.2–63.9%), depending on the technology. An amine-based post-combustion CCS unit was evaluated hydraulically in Aspen HYSYS, operation at low loads resulted in a high regeneration duty of 6100 kJ/kgCO_2. Pre-combustion CCS achieved higher overall CO_2 capture rates than the amine Post-combustion CCS system, albeit at greater CAPEX. The general arrangement and ship characteristics of a reference Panamax-class bulk carrier were used to plan the integration of CCS units and fuel containment systems. Results showed that optimised space utilisation avoided excessive cargo loss for most alternatives, except electricity that could reduce cargo capacity by over 30% due to the low battery energy density. Technical, environmental, and economic assessments identified green fuels, biofuels, and CCS as the most practical long-term options for regulatory compliance and operational sustainability.

1. Introduction

Shipping contributes approximately 3% of global greenhouse gas (GHG) emissions (World Economic Forum, 2022). In response to tightening international regulations, the maritime industry is under increasing pressure to decarbonise. A wide range of strategies has been explored to meet near- and mid-term emission reduction targets, including energy efficiency improvements, voyage optimisation, alternative fuels (e.g., LNG, methanol, hydrogen, ammonia, biofuels), and onboard carbon capture system (OCCS) (IMO, 2023a; Law et al., 2021).

While LNG-powered vessels represent 5.96% of the total global fleet tonnage (Tuswan et al., 2023), the uptake of other low-carbon technologies remain limited (Bayraktar et al., 2024). Selecting suitable retrofit options is particularly challenging due to the diverse vessel types, varied operational patterns, and the fast-evolving landscape of decarbonisation technologies. Some shipowners have already made substantial investments in converting vessels to run on alternative fuels (Lin, 2022; Hand, 2022), or in installing OCCS (Prevljak, 2024; Bureau Veritas, 2023). Numerous techno-economic assessments have evaluated the viability of such technologies for future fleets (Korberg et al., 2021), however, most of these studies rely on static assumptions and do not incorporate real-time operational and fuel consumption data (Kanchiralla et al., 2023).

In conventional ship design approach, retrofits designs are based on generic design conditions or worst-case scenarios, often leading to overdesign and excessive capital investment. For example, a standard sea margin of 15–20% is typically added to ship power to account for

* Corresponding authors at: Cambridge Centre for Advanced Research and Education in Singapore (CARES), CREATE Tower, 1 Create Way, 138602, Singapore.
E-mail addresses: lcl38@cam.ac.uk (L.C. Law), em257@eng.cam.ac.uk (E. Mastorakos).

https://doi.org/10.1016/j.egyr.2026.109610
Received 11 October 2025; Received in revised form 30 June 2026; Accepted 13 August 2026

Nomenclatures

ACAPEX	Annualised capital cost
AE	Auxiliary engine
BLUE	Fuel derived from natural gas
CAPEX	Capital cost
$CAPEX_{New}$	CAPEX of new plant
$CAPEX_{Ref}$	CAPEX of reference plant
CAR	Cargo attainment rate
CCGT	Combined cycle gas turbine
CCS	Carbon capture and storage
C_f	Fuel carbon emission factors
$C_{f,CO2}$	TTW CO_2 emission factor
$C_{f,CH4}$	TTW CH_4 emission factor
$C_{f,N2O}$	TTW N_2O emission factor
$CO_{2,base}$	CO_2 emission from reference ship
$CO_{2,captured}$	Amount of CO_2 captured
$CO_{2,emit}$	Amount of CO_2 emitted
C_{slip}	Methane slip factor
CH_4	Methane
CII	Carbon Intensity Indicator
CO_2	Carbon dioxide
COG	Carbon Intensity Indicator
C_S	Specific cost
C_{total}	Total cost
DCS	Data Collection System
DG	Diesel engine
E	Electricity pathways
E_{fuel}	Total energy demand in MJ
E_S	Specific energy
EEDI	Energy Efficiency Design Index
ETS	Emissions trading schemes
EU	EU Council Regulation
FC	Fuel Cell
FC_{OCCS}	Fuel consumed to meet OCCS demand
FC_{ship}	Fuel consumption of reference ship
FC_{total}	Total overall fuel consumption
GFI	GHG fuel intensity
GHG	Greenhouse gaseous
GHG_{TTW}	TTW emissions factor
GHG_{WTW}	WTT emissions factor
GHGIE	GHG Intensity of Energy
GWP	Global warming potential
H_2	Hydrogen
HFO	Heavy fuel oil
HVO	Hydrotreated vegetable oil
ICE	Internal combustion engine
IMO	International Maritime Organisation
ILUC	Indirect land-use change
IMO	International Maritime Organization
LHV	Lower heating value
LNG	Liquefied Natural Gas
MDO	Marine Diesel Oil
ME	Main engine
MeOH	Methanol
MEPC	Marine Environment Protection Committee
m_{fuel}	Mass of fuel required
NH_3	Ammonia pathway
OCCS	Onboard carbon capture and storage
OP	Operational profile
OPEX	Operating cost
PO	Pure oil
PostCCS	Post-combustion CCS
PreCCS	Pre-combustion carbon capture
PSA	Pressure swing adsorber
PVO	Pure vegetable oil
ROI	Return on investment
ShaPoLi	Shaft Power Limitation
SMR	Steam methane reformer
S_{New}	Capacity of new plant
SOG	Speed over ground
S_{Ref}	Capacity of reference plant
SOLAR-E	Fuel produced using solar electricity
TCS	Tank Connection Spaces
TRL	Technology readiness level
TTW	Tank-to-Wake
TTW_{CO2eq}	Total TTW equivalent emissions
V_{fuel}	Volume of fuel required
WGS	Water gas shift reactors
WTT	Well-to-Tank
WTW	Well-to-Wake
ρ_{fuel}	Density of fuel

uncertainties and ensure operational safety (Geus-Moussault et al., 2024). While this approach is conservative, it may significantly reduce cargo capacity, impact ship layout, and the feasibility of advanced fuel systems, especially those requiring specialised storage tanks such as cryogenic or pressurised tanks. To address this, data analytics on historical dataset at the pre-design stage which could enable a more accurate estimation on power and fuel requirements could help.

The data-driven assessment has been enabled with International Maritime Organisation (IMO) Data Collection System (DCS) and the European Union's MRV Regulation, which require ships of 5000 gross tonnage and above to report fuel consumption and carbon dioxide (CO_2) emissions (MEPC, 2016; IMO, 2025). These datasets facilitate voyage-based analyses, enabling more precise estimates of energy demand and operational patterns. In particular, the use of ship historical data enables improved fuel consumption estimation by accounting for the real corrections for power loss resulting from weather disturbances, ship hydrodynamic, propeller inefficiencies, and other ship resistance factors caused by fouling and vessel aging.

Several studies have demonstrated the potential of such data-driven approaches in optimising ship performance, reducing fuel consumption and emissions (Martinić-Cezar et al., 2024). Examples include predictive models for fuel consumption and CO_2 emissions (Zhang et al., 2024a; Zervos and Themelis, 2021), leg-based assessment for voyage optimisation (He et al., 2024), and the growing application of artificial intelligence and machine learning techniques in maritime analytics (Kim et al., 2026). For instance, Negar et al (Azemati et al., 2025)., Zhang Ruan et al (Ruan et al., 2025). and others have utilised historical ship data to develop machine learning-based fuel consumption prediction models, which can subsequently support energy efficiency optimisation and operational decision-making. These developments highlight the increasing role of data-driven methodologies as a key enabler of ship decarbonisation strategies.

Despite growing interest in data-driven optimisation, many low carbon ship designs, whether for newbuilds or retrofits is lacking integration with actual operational profiles and fuel consumption patterns. This gap may result in suboptimal or overly conservative designs, particularly when applied to vessels with unique or variable voyage characteristics. This study aims to bridge the gap by using two years of historical operational data to derive a detailed operational profile, fuel consumption and emissions profiles of a reference bulk carrier. By analysing voyage frequency, bunkering intervals, operational modes (e.g., sailing, idling, manoeuvring), and emission profiles, this approach allows for a more accurate and operationally aligned conceptual design for reference bulk carrier retrofit with various low-carbon fuel alternatives including (LNG), hydrogen (H_2), ammonia (NH_3), methanol (MeOH), electricity (E), biodiesel, and OCCS. This data-driven approach facilitates the identification of feasible low-carbon retrofit solutions that are tailored to the ship's real-world performance: reducing overdesign, avoiding high capital cost (CAPEX) investment, and enhancing long-term economic sustainability. This holistic approach can also be applied for any vessel to enable shipowners in investing in a right low-carbon solution to decarbonise, without compromising the vessel's profitability.

The key objectives are:

1. To analyse historical operational data of a reference bulk carrier to derive the vessel's operational profile, fuel consumption, and emissions pattern.
2. To apply the above findings to the conceptual design of a low carbon retrofit.
3. To assess and select promising low carbon solutions while eliminating unsuitable alternatives.

This data-driven approach ensures that the retrofit strategy is not only technically sound but also economically viable and aligned with real-world operations. Due to the special interest in OCCS from the maritime industry (DNV, 2024; Wärtsilä, 2022) and the inherently variable load conditions of ship operation, Aspen modelling of Post-Combustion CCS system is included here to evaluate its performance across varying operation conditions. The remainder of this paper is structured as follows: 2 presents the research methodology, 3 discusses results and key findings, and 4 provides conclusions and recommendations.

2. Methodology

2.1. Research approach

In this study, a historical dataset generated by the onboard high-frequency monitoring system, provided by Laskaridis Shipping Co. Ltd. and METIS Space, was analysed. The use of historical operational data enables a better understanding of operational inefficiency based on past voyages record. The derived voyage pattern and fuel consumption

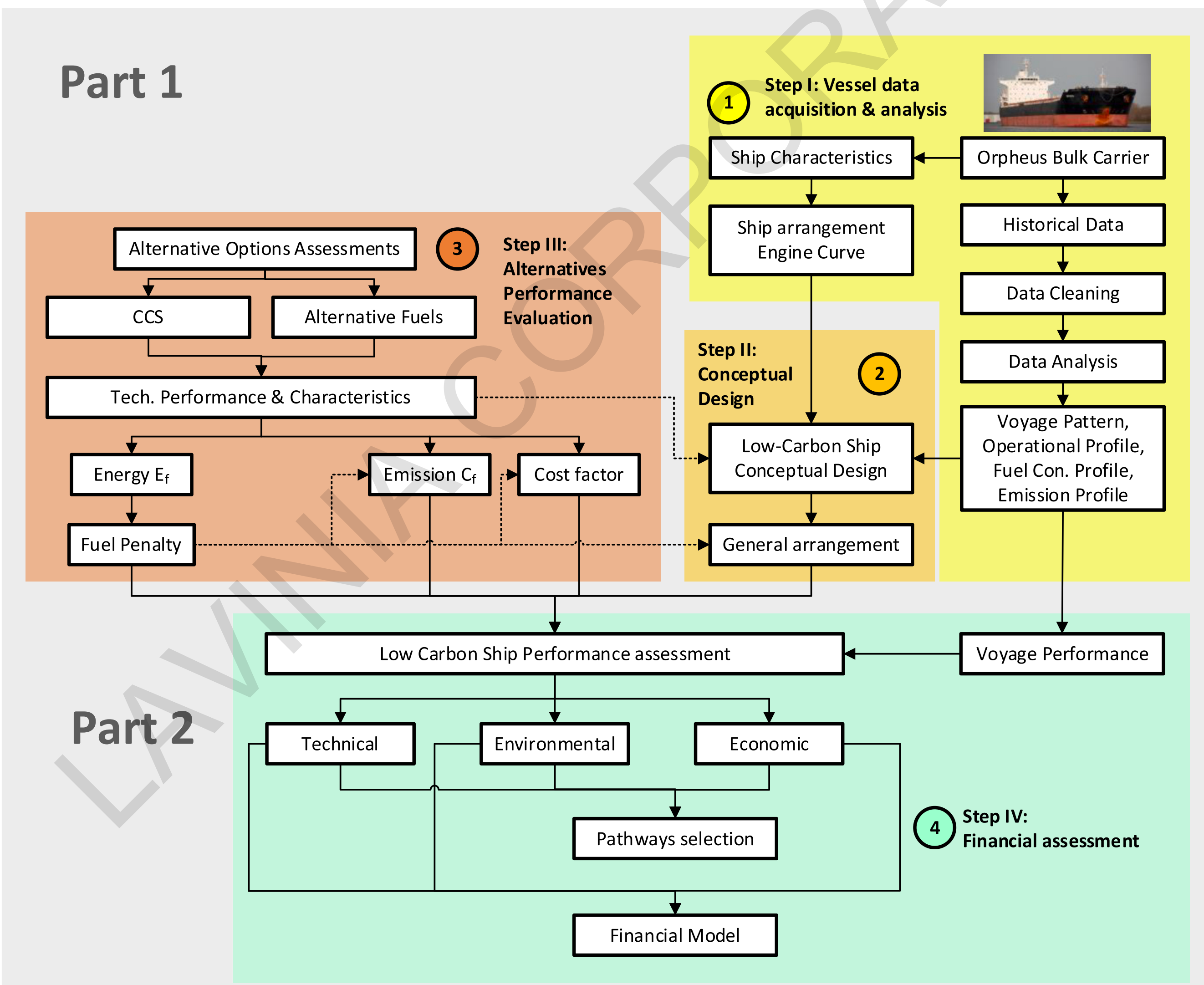

Fig. 1. Research flow diagram divided into two parts. This paper covers the first part (Step I, Step II, and Step III) that focuses on conceptual design of various low carbon ships. The insights obtained from Step I are used in conceptual design in Step II, and Step III evaluate alternative options performances based on the energy factor (E_f) to determine fuel penalty, emissions factor (C_f) and cost factor. In the companion paper (Part 2), the obtained information is used to assess the technical, environmental and economic performance of the reference vessel retrofitted with different low carbon solutions.

profiles were then integrated with alternative fuels and the ship model to ensure that low-carbon ships are not designed solely based on fuel properties, but are tailored to the reference ship. The alternative pathways included in this study include LNG, H_2, NH_3, MeOH, biodiesel, electric propulsion and OCCS. Additionally, a novel concept of OCCS integrating hydrogen production onboard with pre-combustion carbon capture (PreCCS) is included as one of the pathways and denoted as SMR-H2(CCS) (Law et al., 2024) (Law et al., 2024). It should be noted that not all of these options are immediately feasible as retrofit solutions, but it is feasible to assume that (large or small) engine modifications could allow the use of the various alternative fuels in the same engine; this is discussed later. Electric propulsion is included in the ship model as a reference case, particularly for scenarios involving full or partial electrification (e.g. port operations).

The study is divided into two parts, the first part focuses on conceptual design, and the second part (companion Part II paper) addresses economic modelling and sensitivity analysis. The overall research approach is illustrated in Fig. 1. In this paper, only the first part of the work is discussed. Step I focused on the analysis of collected data, including historical data, ship arrangement drawings and engine datasheets. In this step, the vessel's operational profile, fuel consumption trends, and voyage patterns were characterised based on recorded historical data, which provided inputs for the conceptual design of low-carbon ship retrofit. Step II involved the conceptual design of the vessels when integrated with low carbon fuels and OCCS. The OCCS and containment systems for alternative fuels were sized for optimal storage capacity. Subsequently, the general arrangement of the reference ship retrofit for different low carbon alternatives was planned. The ship layout, vessel stability and safety features are also discussed in this study. Step III involved comparative assessment of low carbon alternatives produced from different pathways. Some unrealistic alternatives were eliminated based on the evaluation. The criteria used for selection of suitable pathways included: (i) low carbon intensity, (ii) cost efficiency, (iii) minimal impact on cargo carrying capacity, and (iv) technical safety.

The conceptual design of the low-carbon alternatives provides a comprehensive view on implications of fuel transition. The results obtained from this study were applied to develop economic model of various low carbon transition scenarios, enabling the identification of the most cost-effective solution for the reference ship. This detailed financial projection is included in a companion paper (Part II).

2.2. Step I: Vessel data acquisition and analysis

2.2.1. Reference ship data

The reference ship in this study is a Panamax-class bulk carrier. Table 1 presents the principal characteristics and dimensions of the examined ship. As shown in Fig. 2, this vessel is mechanically propelled with a 9.5 MW main engine connected to a shaft power limitation (ShaPoLi). The power needs for ballast pumps, main engine pumps and accommodation are met by three 600 kW diesel generators serving as

Table 1
Ship particulars and specifications of reference Panamax-class bulk carrier.

Criteria	Symbol	Magnitude (unit)
Length overall	L_{OA}	224.9 m
Length between perpendiculars	L_{PP}	217.0 m
Breadth	B	32.25 m
Depth	T	19.7 m
Block coefficient (@ Design draft)	C_B	0.8616
Forward draft (Ballast/Laden)	T_F	5.0 / 12.2 m
Aft. Draft (Ballast/Laden)	T_A	7.8 / 12.2 m
Contract/Service ship speed	$VS_{contract}$	14.5 knots
M/E type, rated power	P	Wartsila5RT-fleX58T-D, 9500 kW
Main engine SMCR power	$P_{ME,MCR}$	9500 kW
Deadweight	DWT	76,000 tons

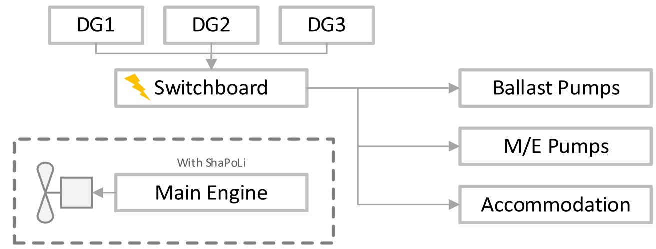

Fig. 2. Block diagram of the propulsion system of the reference ship with a mechanically propelled shaft connected to main engine (ME). Electrical power is generated by three 600 kW diesel generator sets (also known as auxiliary engine, AE), which are connected to a central switchboard for power distribution. The switchboard supplies electricity to essential onboard loads, including ballast pumps, main engine auxiliary systems, and accommodation (hotel) loads.

auxiliary engines. Built in 2016, the reference CII for the reference bulk carrier is 4.382 gCO_2/ton.nm. Given the potential operational lifespan of 25 years, modifications are required to comply with stringent emissions regulations and to avoid penalties.

The reference ship is equipped with a comprehensive sensor network, including GPS, anemometers, torque meters, flow meters, thermometers, gyrocompasses, etc. In total, 268 parameters are recorded, covering navigation data (e.g., speed, heading, and course), vessel operational conditions (e.g., draft and trim), engineering system performance (e.g., fuel oil flow rate, engine power, and rotational speed), and metocean conditions (e.g., wind, wave, and swell characteristics, as well as atmospheric pressure and temperature).

The reference vessel has a total deadweight capacity of 75,631 tons, including 3161.7 tons of non-cargo deadweight, comprising the deadweight for fuels, lubricating oil, freshwater and other miscellaneous items. Hence, the cargo deadweight (DW_C) is approximately 72,469 tons. The cargo volume capacity is 91,939 m^3, with existing fuel tanks totalling 2450 m^3 (2400 tons, 0.98 ton/m^3). With a typical cargo density of 1–1.25 ton/m^3, the vessel is weight-limited (Law et al., 2022). The 72,469 tons of cargo deadweight requires 72,469–90,586 m^3 of volume. This leaves an unutilised cargo space of at least 1350 m^3. This provides the option to renovate the excess space into fuel or CO_2 containment space.

The vessel's general arrangement (Fig. 3) indicates that the current fuel oil tanks are divided into five compartments, with the main tank above the engine room and four additional tanks positioned between the cargo holds and below deck for optimised space utilisation. However, edge spaces marked in grey (Fig. 3(b)) could not accommodate alternative fuels requiring specialised Type C tanks (e.g., hydrogen, LNG). In contrast, the primary fuel tank near the engine room (385 m^3) could be designed to accommodate different fuel types.

In general, a bulk carrier has limited space above deck as the majority of the deck space comprise the hatches for cargo tanks and full accessibility to the hatches is required. Hence, most demonstration projects utilise the deck space at aft zone for fuel tank placement (Riviera News, 2023; gCaptain, 2017). Additionally, the space at the port and starboard closed to the cargo hatches can be optimally utilised to locate storage tanks. For ease of installation, a standard tank size was selected considering ship dimension. As shown in Fig. 4, standard Type C cylindrical tanks with radius of 3 m and length of 16 m (providing storage capacity of approximately 450 m^3) were arranged on both Port and Starboard of the reference vessel. Based on the general arrangement of reference ship, approximately 12 tanks could be installed, offering a total storage capacity of 5400 m^3. In addition, the space available at the aft side was considered for installation of additional tanks or for housing PostCCS and PreCCS plants. By utilising the space above the main deck, the integration of new equipment and tanks could be achieved without affecting the vessel's cargo carrying volume. However, if the required

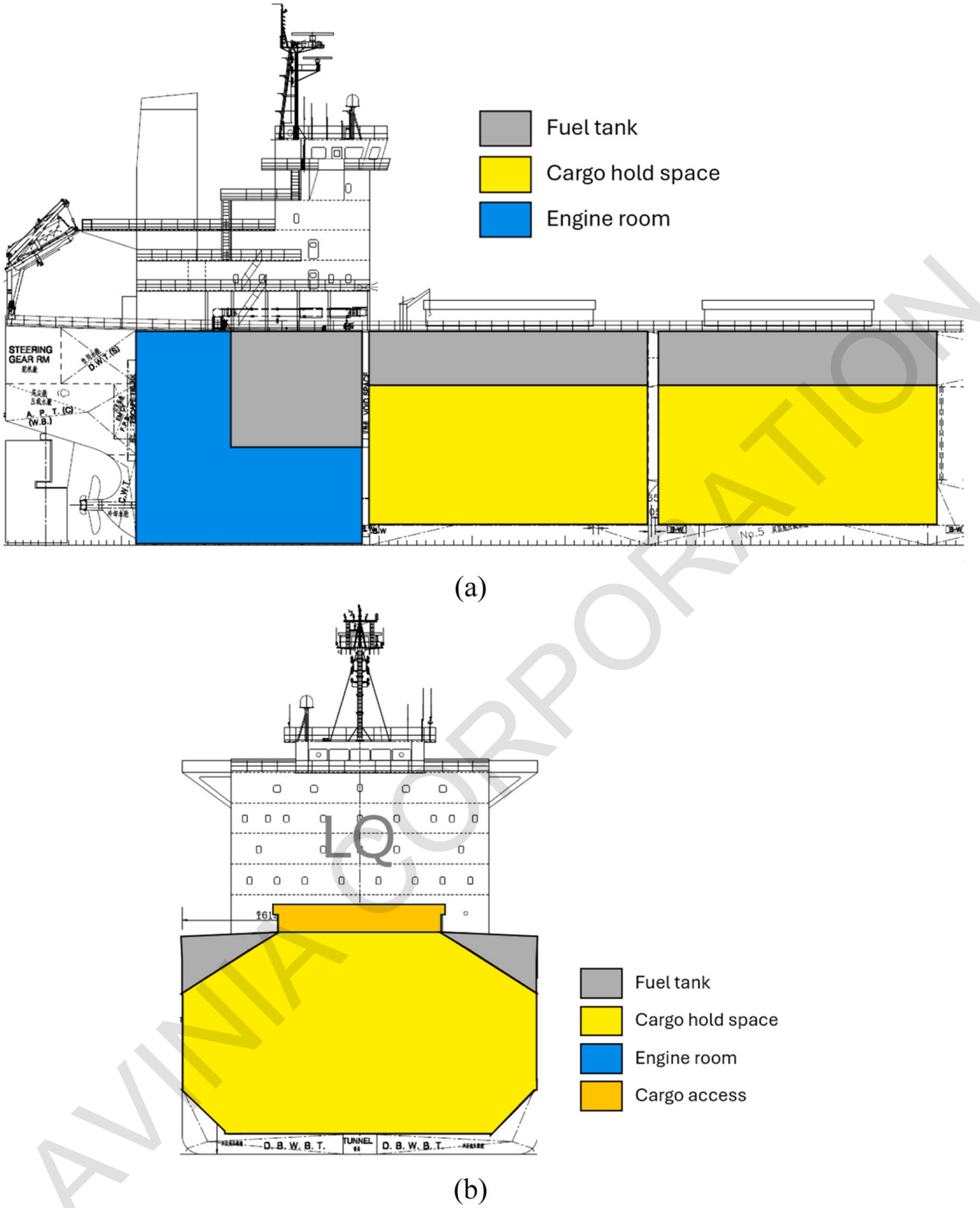

Fig. 3. Ship general arrangement (a) profile view (aft section), and (b) mid-ship section.

space exceeded the available free space, cargo space is assumed displaced, thereby reducing the cargo carrying capacity and indirectly impacting operational revenue.

2.2.2. *Historical data classification*

A two-year dataset contains 268 parameters was collected between January 2023 and December 2024 at a one-minute sampling interval, totalling 1064,161 data points. Data cleaning and preprocessing was performed using Python and Power BI applications. First, raw data CSV files were merged, followed by data inspection and parameter selection to identify relevant variables. The variable names are standardised. Approximately 1% of the dataset was removed due to missing or invalid values in key variables. This proportion is considered sufficiently small to have a negligible impact on the representativeness of the dataset. For continuous time-series variables, short gaps were implicitly smoothed through the 60-minute aggregation process, reducing the impact of transient missing data on the overall analysis.

Additional parameters were derived, including total fuel consumption (MDO and HFO) for each engine, total energy consumption, total power output, travelled distance between timestamps, CO_2 emissions, and overall system efficiency (Aggregated data is included in Appendix A, Table A1). The processed dataset was then analysed using speed-over-

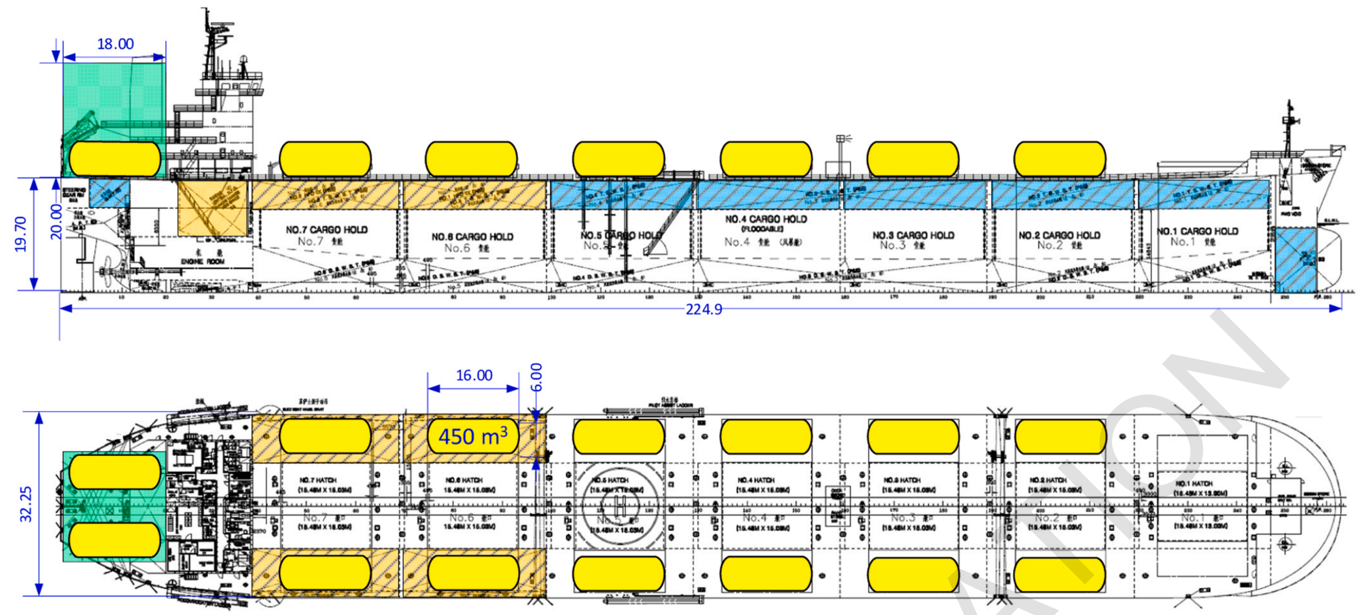

Fig. 4. Ship general arrangement with reserved volume for fuel containment system and placement of OCCS or other equipment. The volume in green is reserved for installation of OCCS plant, the cylindrical volume in yellow is reserved for storage of fuel and captured CO_2. The shaded areas represent the existing fuel tanks on board the vessel.

ground (SOG)-based binning. Operational statistics, including time distribution, average main engine (ME) and diesel generator (DG) power, and average fuel consumption, were computed for each speed bin. These outputs were used to derive the ship's operational profile, fuel consumption trends, and emissions profile.

Before developing the operational profile, voyage modes were classified accordingly to the definitions in Table 2, based on speed over ground (SOG) and draft height. Speeds below 3 knots were categorised as low-speed operation, while speeds of 3 knots and above were considered sailing. Sailing operations were further classified into ballast and laden conditions based on forward draft, where voyages with a forward draft of ≥ 10 m were classified as laden, while the rest were considered ballast. When the vessel was stationary (SOG = 0), it was classified as operating in idle mode. The overall data preprocessing and analytical workflow is illustrated in Fig. 5. This structured workflow ensures that the derived profiles are directly representative of the vessel's real operational behaviour.

The data analysis and visualisation show that the bulk carrier operates across a wide range of speeds and power demands, due to the dynamic behaviour of external conditions such as wind and waves effects and also influenced by varying operational modes (loading, unloading, laden, ballast, drifting and idling). The data-driven approach enables a better understanding of vessel performance under varying conditions and modes.

2.2.3. Ship operational profile, fuel consumption and emission models

The ship operation profile was developed as a simplified chart comprising: (i) percentage of time spent within specific speed ranges across different voyage modes, and (ii) the average power demands for propulsion and electricity loads under varying conditions. Fig. 6 shows

Table 2
Voyage modes classification.

Voyage mode	Speed of ground, SOG (knots)	Draft, T (m)
Idle (At port)	SOG = 0	Any range
Drift (At port)	0 < SOG < 3	Any range
Laden	SOG ≥ 3	T ≥ 10
Ballast	SOG ≥ 3	T < 10

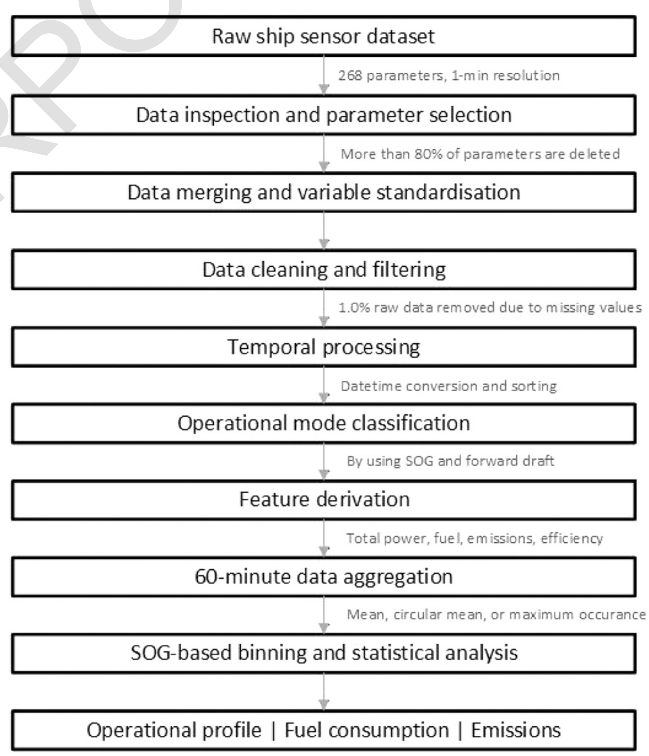

Fig. 5. Workflow of data preprocessing and analytical processing for deriving ship operational, fuel consumption, and emissions profiles. The raw ship sensor dataset (268 parameters at one-minute resolution) was first inspected to identify relevant variables. The data were then merged, standardised, and cleaned, with approximately 1% of records removed due to missing or invalid values. Temporal processing and operational mode classification were performed based on speed over ground (SOG) and draft. Subsequently, key performance variables were derived, and the dataset was aggregated into 60-minute intervals using variable-specific methods. Finally, SOG-based binning and statistical analysis were applied to generate the operational, fuel consumption, and emissions profiles.

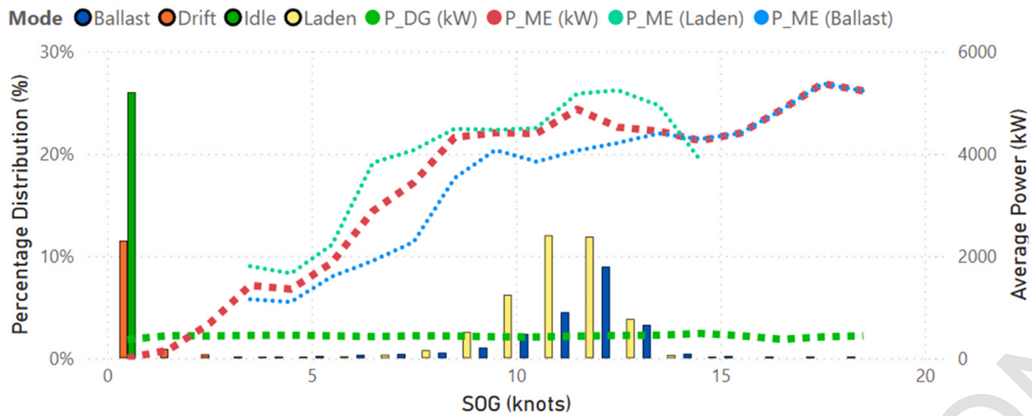

Fig. 6. Operational profile of reference bulk carrier in 2024. The bar chart (left axis) shows the percentage time distribution of each operational mode (Ballast, Laden, Drift, and Idle) across different speed over ground (SOG) bins. The lines (right axis) represent the average power generated by the main engine (P_ME) and diesel generators (P_DG) as a function of SOG. The main engine power profiles at laden and ballast conditions are shown separately as P_ME (Laden) and P_ME (Ballast).

the operational profile (OP) of the reference ship for the year 2024, visualised using a bin size of 1 knot SOG. Next, the fuel consumption profile of the reference vessel for 2024 is shown in Fig. 7, and the ship's emissions profile was derived by multiplying the fuel used with standard carbon emission factors (C_f), as illustrated in Fig. 8. These figures also highlight how fuel consumption rates vary across speed modes,

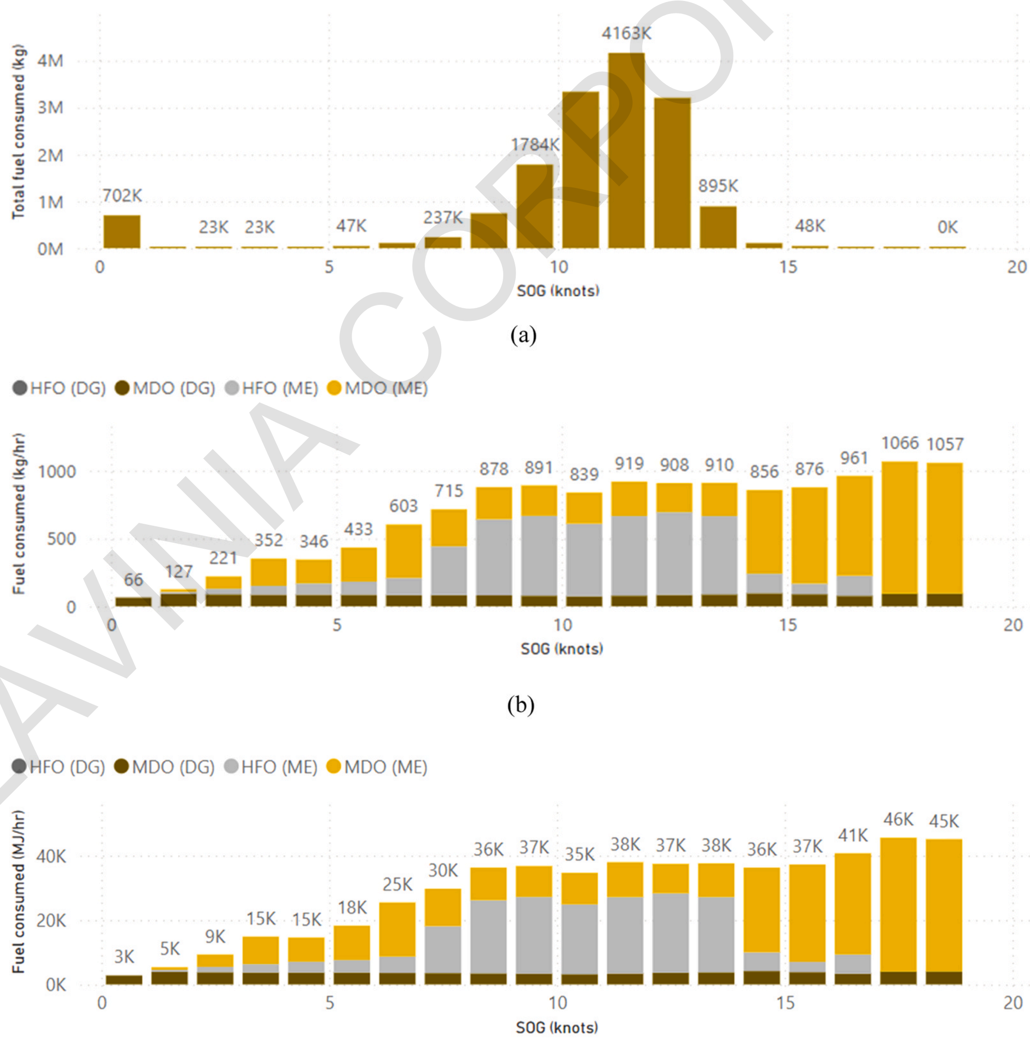

Fig. 7. Fuel consumption profile of the reference bulk carrier in 2024 (a) total fuel consumption at different speed bins, (b) hourly rate of fuel (both HFO and MDO) consumptions in kg/hr, and (c) hourly rate of fuel consumption (both HFO and MDO) in MJ/hr.

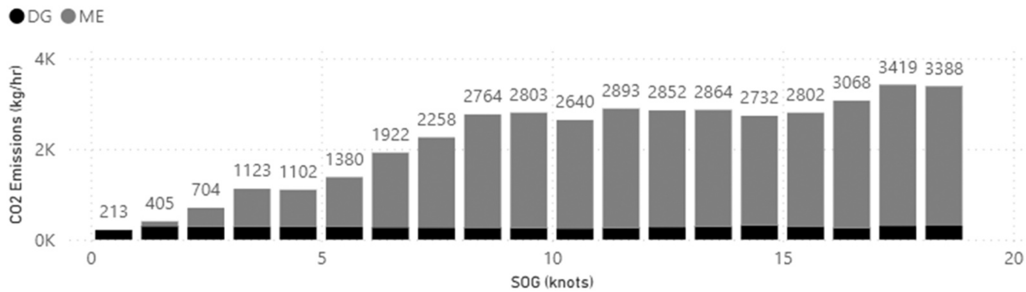

Fig. 8. CO_2 emissions (from both main engine and diesel engines) profile of reference bulk carrier in 2024.

underlining the importance of considering part-load operation in the analysis. Based on these insights, the total fuel consumption and emissions were projected for scenarios in which the vessel operated on alternative low carbon solutions and the optimal capacity of carbon capture is decided. Subsequently, the conceptual design of the low-carbon ship was carried out.

2.3. Step II: Conceptual design of future ship

In this section, the OCCS and fuel containment system conceptual design and layout planning are described.

2.3.1. Conceptual design of amine-based post-combustion CCS

With reference to the existing OCCS studies (GCMD; Stena Bulk; OGC, 2024), most systems were designed based on emissions rates at maximum continuous rating (MCR) (Juliana Monteiro, Research Scientist at TNO, 2020; Luo and Wang, 2017; Ros et al., 2022; OGCI et al., 2021; Lee et al., 2021; Oh et al., 2024; Awoyomi et al., 2019; Long et al., 2021). Feenstra et al. highlighted that designing OCCS based on 100% load leads to oversized system (Feenstra et al., 2019). Moreover, evaluating ship CII and EEDI using a single operating state tends to overestimate carbon reduction potential, as it overlooks part-load operations (Oh et al., 2023). Stec et al (Stec et al., 2021). considered only 35–68% of exhaust gas feed into absorber to achieve 31.4–56.5% CO_2 recovery. Some studies focused on exhaust from main engine only (Stec et al., 2021), while others included both main and auxiliary engines. In several studies, the CO_2 recovery rate was limited by available recoverable heat or the cold energy from LNG evaporation (Ayachi et al., 2025), which could be integrated for CO_2 liquefaction. These approaches lead to more compact CCS installation (Bureau Veritas, 2023). However, most existing studies did not evaluate OCCS performance under part-load operation (GCMD; Stena Bulk; OGC, 2024). As highlighted in the REMARCCABLE project (GCMD; Stena Bulk; OGC, 2024), amine-based CCS was operated only when the flow rate reached at least 30% of design capacity, constrained by downstream equipment that cannot handle large turndown ratios. Accounting for these operational limits is therefore crucial when designing realistic OCCS system (Oh et al., 2023).

In this study, post-combustion CCS (Post-CCS) was retrofitted to the reference ship fuelled by both HFO and for the alternative option with LNG. For HFO(CCS), the CO_2 capture rate and energy penalty from (GCMD; Stena Bulk; OGC, 2024) were used. For the LNG-fuelled case, a detailed design was developed based on the validated MEA/MDEA blended amine system (Law et al., 2017a, 2017b). The vessel operational profile (Fig. 6) was analysed and optimal CCS capacity was determined. The LNG(CCS) was sized to handle the peak exhaust flow during laden operation (11–12 knots), and the system was set to operate between 30–100% load. CO_2 liquefaction employed an ammonia-based refrigerant integrated with a compression-expansion process, and OCCS power demand was assumed to be fully met by existing auxiliary engines, leading to increased fuel consumption. Consequently, the vessel performance with CCS under varying load conditions was evaluated as an integrated system (Fig. 9).

The combined OCCS and CO_2 liquefaction system (Fig. 9) was simulated using Aspen HYSYS. The Aspen model and key inputs for the OCCS are shown in the Appendix Figure D1 and Table D2. MEA/MDEA blended amine is utilised for improved regeneration duty. The absorber and regenerator columns were sized based on the designed capture capacity, and part-loads operation was subsequently evaluated using the sized columns. A hydraulic analysis (Fig. 10) was performed to assess columns performance under turndown conditions and discovered that higher regeneration duty and amine circulation rate was needed when the CCS is operated at lower operational load, to avoid operation below flooding at different column stages. The simulation results were integrated with the vessel's operational profile to quantify additional fuel and power demands at different operating speeds. The design process was iterative, as the CCS inlet flows depends on both main engine and auxiliary engine exhaust, while auxiliary engine load is affected by CCS-related demands including amine circulation, CO_2 compression, and liquefaction.

CAPEX ($CAPEX_{New}$) was estimated using the six-tenths rule (Eq. 1), with a reference plant cost of $14.7 million at 1286 $kgCO_2/hr$ capture capacity, taken from (GCMD; Stena Bulk; OGC, 2024). The parameter S (Eq. 1) represents the plant capacity, in this case CO_2 capture capacity. Based on the conceptual design, the PostCCS performance was evaluated by calculating the total fuel consumption (Eq. 2), energy or fuel penalty (Eq. 3), and CO_2 capture efficiency (Eqs. 4–5).

From Eq. (2), total fuel consumption (FC_{total}) is determined by summing the additional fuel required by the CCS reboiler (FC_{OCCS}) and the baseline fuel consumption of the reference ship (FC_{ship}). The energy penalty of OCCS is defined as the percentage of added energy consumed to the initial energy consumption of the reference ship, Eq. (3). The total energy requirement was calculated by multiplying the amount of fuel consumed by the fuel's lower heating value (LHV). The gross CO_2 capture measure the carbon capture effectiveness of CCS, dividing the amount of CO_2 captured with total emissions. While gross CO_2 capture indicates the system's removal performance, the net CO_2 reduction provides a more meaningful measure by accounting for the net CO_2 reduced ($CO_{2,base}$ minus $CO_{2,emit}$) as compared to the emissions of the reference vessel without CCS ($CO_{2,base}$) (Sari and Kolmetz, 2014).

$$CAPEX_{New} = CAPEX_{Ref} \times \left(\frac{S_{New}}{S_{Ref}}\right)^{0.6} \tag{1}$$

$$\textit{Total fuel consumption}, \quad FC_{total} = FC_{ship} + FC_{OCCS} \tag{2}$$

$$\textit{Fuel penalty}(\%) = \quad \textit{Energy penalty} \quad (\%) = \frac{(FC_{OCCS}) \times LHV}{FC_{ship} \times LHV} \times 100\% \tag{3}$$

$$\textit{Gross } CO_2 \textit{ capture rate} \quad (\%) = \frac{\textit{Amount of } CO_2 \textit{ captured}, \quad CO_{2,captured}}{\textit{Emission from reference}, \quad CO2_{Base} \quad + \textit{additional emissions}} \times 100\% \tag{4}$$

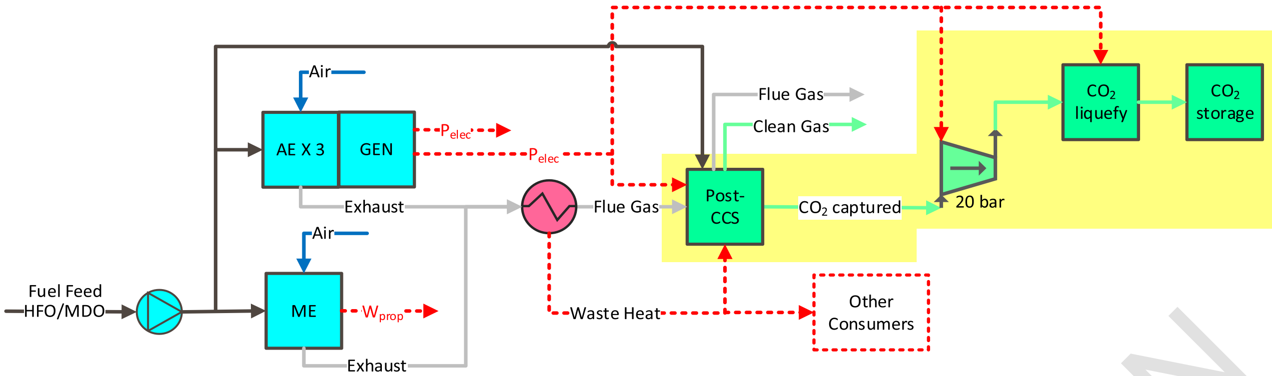

Fig. 9. Ship-based onboard carbon capture system to treat exhaust from both AE and ME, and the additional power needs of CO_2 compressor, CO_2 liquefaction system and amine-based post-combustion CCS were supplied from AE.

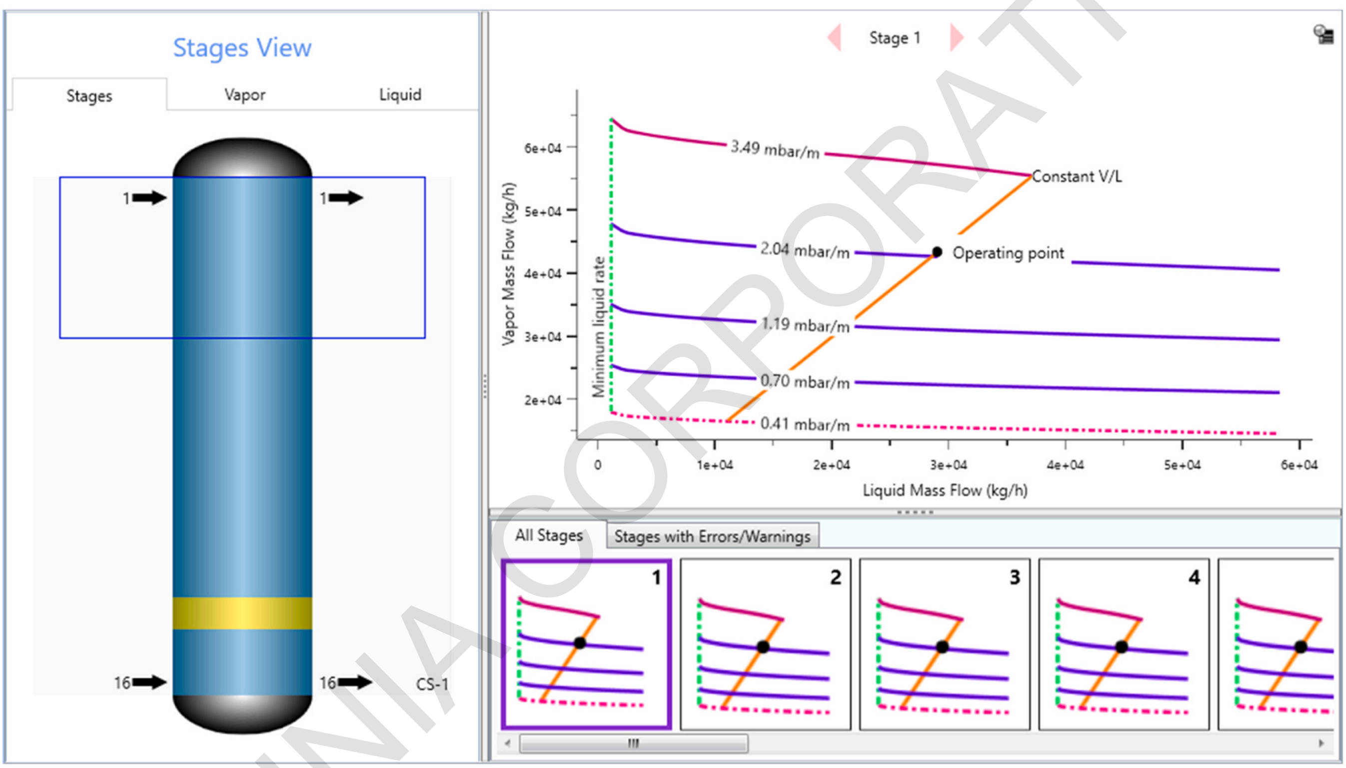

Fig. 10. Hydraulic plot from Aspen HYSYS for absorber column showing the operating point in relation to flooding and weeping limits. Yellow-highlighted stages indicate operation close to hydraulic constraints. The design is based on published work (Law et al., 2017a, 2017b), a CCS with blended MEA/MDEA amine as sorbents. More detail about the Aspen model is presented in Appendix D (Fig. D1, Table D2).

$$\textit{Net } CO_2 \textit{ reduction rate } (\%) = \left(1 - \frac{\textit{Total emission after } CO_2 \textit{ captured}, \quad CO_{2,emit}}{\textit{Emission from reference}, \quad CO_{2,base}}\right) \times 100\% \tag{5}$$

2.3.2. *Conceptual design of steam methane reformer (SMR) with pressure swing adsorber (PSA) for pre-combustion CCS (Pre-CCS)*

The conceptual design for Pre-combustion CCS builds on preliminary work on a PreCCS system builds upon prior work (Law et al., 2024), in which an integrated system comprising a steam methane reformer (SMR), water gas shift reactors (WGS) and pressure swing adsorber (PSA) was developed and validated against experimental data. The integrated system is further coupled with an intensive waste heat recovery (WHR) network to achieve optimal heat utilisation. The detailed Aspen model of the PreCCS system is presented in Appendix D (Fig. D3) and the key input and simulation output for the model is summarised in Appendix D (Table D4). This applies to LNG only (reforming HFO is not considered).

The SMR-WGS-PSA unit was integrated with a combined cycle gas turbine (CCGT) propulsion system to enhance operational flexibility and accommodate wide range of reformate compositions, turning the ship into an electrically-propelled vessel. As previously studied in Ref (Law et al., 2024)., the baseline PreCCS configuration achieved a CO_2 capture rate of 61.33%, with a reduction in net efficiency of CCGT from 51.6% to 41.5% when the heat demand is supplied via direct methane combustion in the reformer furnace. Building on the baseline design, the system configuration is modified by utilising hydrogen-rich reformate as fuel for the SMR furnace, thereby improving the overall CO_2 capture efficiency from 61.33% to 82.82%, albeit with increased fuel consumption. The modified configuration is illustrated schematically in Fig. 11. In this study, the integrated system is referred as SMR-H2(CCS). The process involves the following stages:

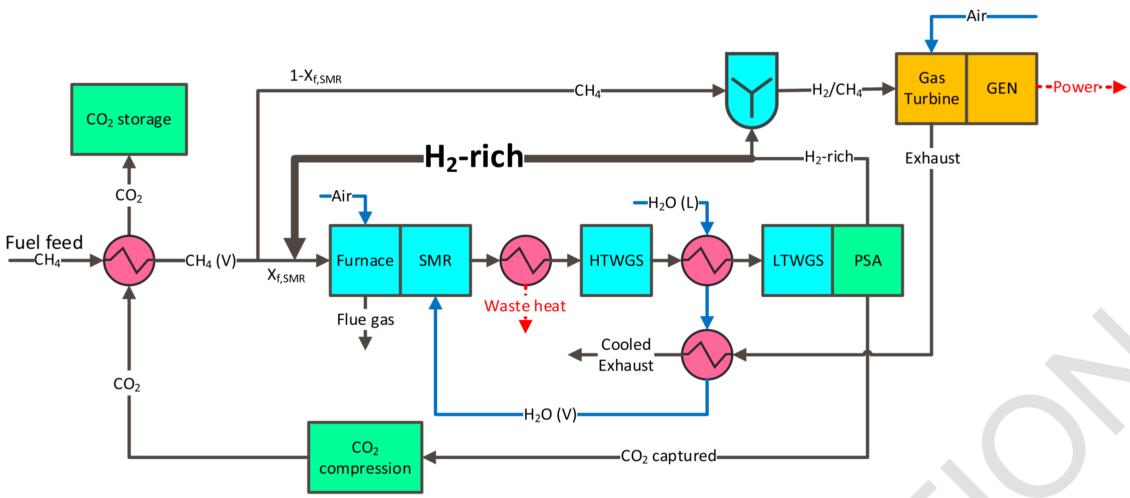

Fig. 11. Reformer system integrated with combined cycle propulsion system. Waste heat from SMR, high temperature WGS and exhaust streams is recovered. Compared to the base SMR-PSA system (Law et al., 2024), the H_2-rich reformate produced in the SMR is also directed to the furnace, reducing the furnace CO_2 emissions (as indicated by the thickened line). More detail about the Aspen model is presented in Appendix D (Fig. D3, Table D4).

i. SMR to convert LNG into syngas;
ii. high- and low-temperature WGS reactions to enhance hydrogen production;
iii. gas purification via PSA using activated carbon adsorbents to separate CO_2 from syngas (90% separation efficiency);
iv. liquefaction and storage of the separated CO_2;
v. use of H_2-rich reformate as fuel for both CCGT and reformer furnace; and
vi. power generation by the CCGT to meet propulsion and auxiliaries demands.

The SMR-H2(CCS) is designed as a modular unit to accommodate fluctuations in onboard energy demand and to ensure operability across the vessel's full fuel range. CAPEX estimates from the IEA (International Energy Agency IEA, 2017; Law et al., 2023a) range between €264–314 million for hydrogen production capacity of 8990 tons/hr, depending on the CCS technology. Using the sixth-tenth rules (Eq. 1), the CAPEX of the proposed plant was estimated by scaling these reference costs. In the absence of detailed equipment sizing, space was allocated in the aft section installation of this hydrogen production module.

2.3.3. *Fuel containment for alternative fuels*

Based on the analysis of total fuel consumption per round-trip between bunkering calls, the total energy demand (E_{fuel}) ranged from 13.2 to 77 million MJ. The longest voyage, lasting approximately four months, required 77 million MJ. Foreseeing that bunkering port would be available along the route, the containment capacity for this study was set at 50 million MJ (design capacity). The containment systems for various fuel types were sized for the design capacity. Then, the mass (m_{fuel}) and volume (V_{fuel}) of each fuel were estimated using Eqs. (6) and (7). The m_{fuel} was estimated by dividing the energy demand (E_{fuel}) with fuel's LHV, and V_{fuel} dividing the mass of fuel with density (ρ_{fuel}).

Table 3 summarises the properties and storage conditions of different fuel types. For biodiesel and methanol, which exhibit properties similar to conventional marine fuel, no major redesign is required to reuse existing diesel fuel tanks. The vessel's existing storage capacity is approximately 2450 m^3 (equivalent to fuel a fuel deadweight of 2400 tons) and was assumed to be available for storing biodiesel and methanol.

In contrast, LNG, H_2 and NH_3 require dedicated tanks with specialised insulation, making reuse of existing tanks infeasible. Among the available containment technologies, IMO Type C and prismatic Type A

Table 3
Properties, storage condition and storage cost factor of selected marine fuels. The majority of the data are adopted from the authors' previous work (Law et al., 2021).

Pathways	LHV Specific Energy (kJ/kg) (EUR-Lex, 2009)	Storage tank type	Storage condition (° C, bar)	Volumetric Density (kJ/m^3) (Law et al., 2021)	Mass Density, ρ (kg/m^3) (Law et al., 2021)	Storage Cost ($/kg LNG Equivalent) (SEA-LNG, 2019)	Storage Cost ($/kJ LNG Equivalent) (Law et al., 2021; SEA-LNG, 2019)
HFO	40,500	Conventional tank	Liquid, 40, 1	40,740,000	970	1.5	3.01×10^{-5}
LNG	49,100	Type C (Fan, 2021)	Liquid, −162, 0	21,341,488	428	3.5 – 7.0 (SEA-LNG, 2019)	1.20×10^{-4}
H2	120,000	Type C (Alkhaledi et al., 2021)	Liquid, −253, 1	9049,200	75	7.0 – 19.5 (SEA-LNG, 2019)	2.41×10^{-4}
NH3	18,600	Type C (Fan, 2021; Dahlke-Wallat et al., 2024)	Liquid, −34, 1	11,055,840	594	3.75	7.52×10^{-5}
MEOH	19,900	Conventional tank	Liquid, 20, 1	15,758,810	792	1.5 – 2.0 (SEA-LNG, 2019)	4.01×10^{-5}
Electricity	1224	Battery	Atmospheric cond.	2434,000	1989	18,500 (SEA-LNG, 2019)	3.71×10^{-1}
Biodiesel	43,000	Conventional tank	Liquid, 25, 1	32,592,735	870	1.5	3.01×10^{-5}
CO_2	-	Type C	Liquid, −20, 20	-	1031 (Carbon Dioxide Properties, 2025)	-	-

membrane tanks are the most mature, with extensive operational track records. Type A tanks are preferred for newbuild vessels, as their integration requires alignment with the ship's construction schedule (Fan, 2021; Alkhaledi et al., 2021; Raucci et al., 2015; Dahlke-Wallat et al., 2024). For retrofit projects, Type C tanks are generally more suitable due to their simpler installation and lower maintenance requirements. The same Type C design is used for storage of fuel and captured CO_2.

2.4. Step III: Low-carbon alternatives assessment

Six types of alternative fuels: LNG, H_2, NH_3, MeOH, Electricity, biodiesel, and four pathways with onboard CCS: HFO(CCS), LNG(CCS), SMR-H2(CCS)*, SMR-H2(CCS) were considered in this study. Each fuel can be produced through various processes and integrated with different propulsion systems, resulting in a wide range of alternative decarbonisation pathways. The SMR-H2(CCS)* represents baseline SMR systems burning methane to generate heat. In a preliminary study (Law et al., 2021), 22 alternative pathways (including both blue and green options) were evaluated from a lifecycle perspective, establishing a database for energy and cost factors across pathways. For the present study, the fuel prices were updated to reflect current market rates. Fuels derived from natural gas are referred to as BLUE fuels, while those produced using renewable electricity (e.g., solar) are referred to as SOLAR-E fuels.

Additionally, both the SMR-H2 and amine-based CCS systems were assessed under part-load operations specific to the OP of the reference ship, and their corresponding fuel penalties and CO_2 reduction factors were estimated. Then, a comparative assessment of the various pathways was carried out from technical, environmental and economic perspectives.

2.4.1. Technical: space, stability and safety (3S) assessment

Space: From the conceptual design, the added mass and volume associated with different low carbon alternatives were estimated. Based on these estimates, storage tank and equipment layouts were developed, enabling an assessment of spatial requirements and the quantification of cargo capacity loss (%) for each alternative.

Stability: For the reference vessel, the initial centre of gravity (COG), metacentric height and metacentric radius were recorded at 17 m, 2 m, and 19 m, respectively. Following the integration of new equipment and storage tanks, these stability parameters must be recalculated to reflect the revised weight distribution. Therefore, the weight and vertical distance from keel to COG of added components including fuel tanks, CO_2 tanks, and CCS plants were estimated. To preserve vessel stability, it was assumed that the added weight of the fuel containment and CO_2 capture systems would be offset by an equivalent reduction in cargo deadweight.

Safety: Each alternative fuel introduces distinct hazards that must be mitigated through risk assessments and appropriate design measures. The design must comply with Class and Statutory requirements, primarily defined by IMO instruments such as SOLAS, MARPOL, and the IGF Code (International Maritime Organisation IMO, 2025), alongside the relevant Class Rules (e.g. ABS (ABS, 2019), DNV, LR (Lloyd's Register, 2025)). These collectively govern the safe arrangement, weight distribution, stability, and fire protection systems for vessels adopting alternative fuels.

2.4.2. Environmental assessment

The IMO and European Commission have implemented regulatory measures and CO_2 reduction targets to regulate GHG emissions from ships. Prior to the 83rd session of IMO's Marine Environment Protection Committee (MEPC) meeting, Carbon Intensity Indicator (CII) was the key regulatory metric introduced by IMO for monitoring ship compliance through CII trajectories (IMO, 2022, 2023b). CII is estimated by dividing the Tank-to-Wake (TTW) emissions with deadweight and distance travelled, Eq. (7). Following MEPC 83 (April 2025), a new metric, GHG fuel intensity (GFI) was introduced. GFI measures Well-to-Wake (WTW) GHG emissions per unit of energy used onboard, expressed in gCO_{2eq}/MJ (Lloyd's Register, 2025). Conceptually, GFI is similar to the GHG Intensity of Energy (GHGIE) under FuelEU Maritime. However, these two metrics differ in compliance reference lines and the associated penalty mechanism, as summarised in Table 4. As shown, GFI targets are defined only up to 2035; extrapolated reduction pathways for 2036–2050 were developed, as presented in Fig. 12.

Both GHGIE and GFI require estimation of WTW CO_{2eq} emissions. As IMO has not yet provided default WTT emissions values for selected alternative pathways, this study adopts default values from EU Council Regulation (EU) 2023/1805 for GHGIE estimation and applies the same for GFI. In addition to GFI and GHGIE regulations, the EU Emissions Trading System (ETS) has also been extended to penalise GHG emissions from ships.

The WTT emissions factor (GHG_{WTT}), TTW emission factors (Cf_{CO2}, Cf_{CH4}, Cf_{N2O}) and methane slip factor (C_{slip}) were sourced from literature and summarised in Appendices A (Table B1). Total TTW equivalent emissions ($TTWCO_{2eq}$) were calculated using Eqs. (8) - (9), multiplying

Table 4
The reduction targets set by European Council and International Maritime Organisation regulations.

Criteria	European Council, Fuel EU (European Parliament and the Council of The European Union, 2023)	IMO, GFI (Lloyd's Register, 2025) (Base Target)	IMO, GFI (Lloyd's Register, 2025) (Direct compliance target)	IMO, CII (IMO, 2022, 2023b)
Reference year	2020	2008	2008	2008
Reference value	91.16 gCO2eq/MJ	93.3 gCO2eq/MJ	93.3 gCO2eq/MJ	Varies
Reduction targets from the reference value at different years (%)	2025 (2%) 2030 (6%) 2035 (14.5%) 2040 (31%) 2045 (62%) 2050 (80%)	2028 (4%) 2029 (6%) 2030 (8%) 2031 (12.4%) 2032 (16.8%) 2033 (21.2%) 2034 (25.6%) 2035 (30%)	2028 (17%) 2029 (19%) 2030 (21%) 2031 (25.4%) 2032 (29.8%) 2033 (34.2%) 2034 (38.6%) 2035 (43%)	2025 (9%) 2030 (21%) 2050 (100%, net-zero emissions)
Required value, 2025 (gCO2eq/MJ)	89.34	-	-	-
Required value, 2030 (gCO2eq/MJ)	85.69	85.84	73.71	-
Required value, 2035 (gCO2eq/MJ)	77.94	65.31	53.18	-
Required value, 2040 (gCO2eq/MJ)	62.90	-	-	-
Required value, 2045 (gCO2eq/MJ)	34.64	-	-	-
Required value, 2050 (gCO2eq/MJ)	18.23	-	-	-
Penalty	€2400/ equivalent metric ton of VLSFO	$100/ ton CO2eq	$380/ ton CO2eq	No penalty was discussed

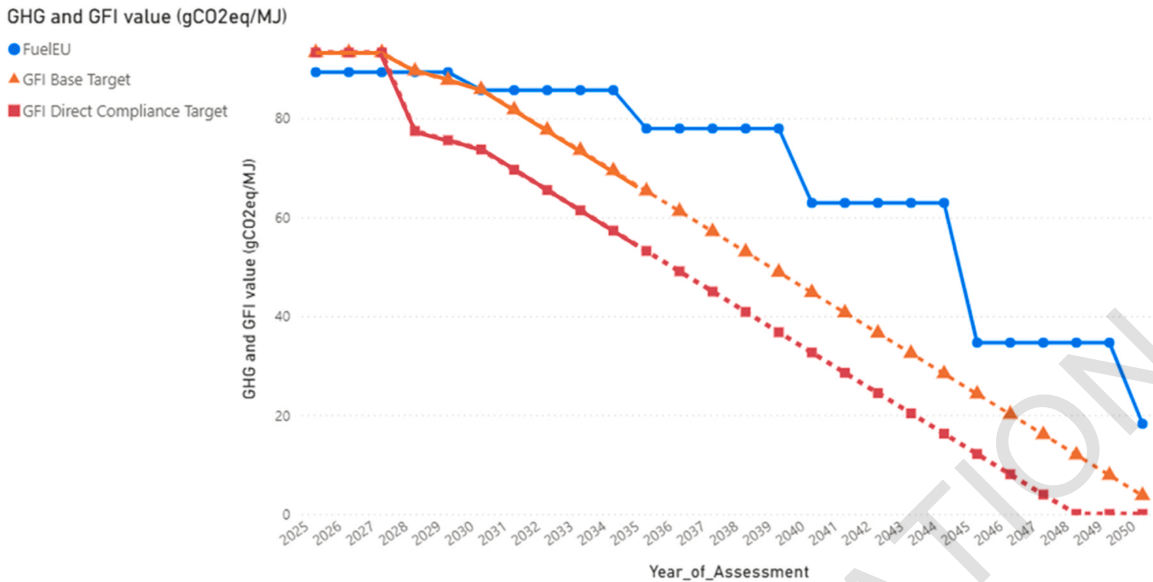

Fig. 12. Comparison of regulatory greenhouse gas intensity trajectories for shipping: FuelEU GHG intensity targets (blue) (European Parliament and the Council of The European Union, 2023), IMO GFI base targets (orange), and GFI direct compliance targets (red), expressed in gCO_2eq/MJ. GFI targets are currently defined up to 2035 (Lloyd's Register, 2025); values beyond 2035 are extrapolated in this study to illustrate potential reduction pathways through 2050.

the 100-year global warming potential (GWP) of 1 for CO_2, 28 for CH_4, and 265 for N_2O with the TTW emission factors, in accordance with IMO Resolution MEPC.376(80) (IMO, 2023c). Next, the GHG_{TTW} emissions factor was calculated using Eq. (10), expressing TTW equivalent emissions relative to fuel energy content. Finally, GHGIE and GFI values were calculated using Eq. (11) by summing GHG_{WTT} with the calculated GHG_{TTW}.

This analysis captures lifecycle emission variations across fuel types and production pathways. For each fuel, both BLUE (fossil-based) and SOLAR-E pathways were considered. Only pathways with GHGIE values lower than the reference were deemed viable low-carbon alternatives.

$$m_{fuel}\ (\text{tons}) = \frac{\Sigma\, E_{fuel}(MJ)}{LHV(MJ/ton)} \tag{6}$$

$$V_{fuel}\quad (\text{m}^3) = \frac{m_{fuel}}{\rho_{fuel}} \tag{7}$$

$$CII = \frac{TTW\ CO_2(gCO2)}{deadweight\quad (tons) \times distance\ travelled\quad (nm)} \tag{7}$$

$$\Sigma\ TTW\ CO_{2eq}(gCO2eq) = \left(m_{fuel} \times \left[\left(1 - \frac{C_{Slip}}{100}\right) \times TTW\ CO_{2eq} + \frac{C_{Slip}}{100} \times GWP_{slip}\right]\right) - m_{CO2\quad captured} \tag{8}$$

$$TTW\ CO_{2eq} = (\text{GWP}_{\text{CO2}} \times C_{f,CO2} + \text{GWP}_{\text{CH4}} \times C_{f,CH4} + \text{GWP}_{\text{N2O}} \times C_{f,N2O}) \tag{9}$$

$$GHG_{TTW}\quad \left(\frac{gCO2eq}{MJ}\right) = \frac{\Sigma\ TTW\ CO_{2eq}(gCO2eq)}{m_{fuel} \times LHV} \tag{10}$$

$$GHGIE = GFI = GHG_{WTW}\quad \left(\frac{gCO2eq}{MJ}\right) = GHG_{WTT}\left(\frac{gCO2eq}{MJ}\right) + GHG_{TTW}\left(\frac{gCO2eq}{MJ}\right) \tag{11}$$

2.4.3. Economic assessment

Ship economic performance and return on investment (ROI) depend strongly on annual operating expenditures (OPEX) and CAPEX investment. With tightening GHG regulations, penalties for exceeding emission limits may significantly increase OPEX. Therefore, a detailed estimation of cost components associated with alternative fuels and onboard CCS integration is essential for informed decision-making. For retrofitting an HFO-fuelled bulk carrier, additional CAPEX is required for fuel containment systems and OCCS units. CAPEX values were annualised using results from the conceptual design (Step II).Fuel prices, which dominate OPEX and exhibit high volatility, were updated using the latest market data:

- **Fossil HFO**: The price of HFO is less volatile than LNG. A higher price was observed in October 2022, at around \$650/MT, while a lower price of below \$450/MT was recorded in May 2025 (Ship and Bunker, 2025; Integr8fuels, 2025). An intermediate value of **\$550/MT** was used.
- **Fossil LNG**: The price of LNG has shown significant volatility. In 2025, prices dropped from around \$1000/MT in February 2025 to \$700/MT in September 2025, whereas in September 2022, prices were higher at \$2600/MT (Ship and Bunker, 2025). **\$800/MT** was used.
- **Blue fuels**: The price of fossil methanol was approximately \$340/MT (Procurement tactics, 2025). The electricity price for extra high-voltage supplies was 12.90 cents/kW (SP Group, 2025), used to revise the fuel costs for BLUE-E pathways without CCS.
- **Biodiesel**: prices vary widely depending on regional feedstock sources such as palm oil, soybean and rapeseed oil. Reported prices range from \$500 to over \$2000/MT (Procurement Resource, 2025). For Fischer-Tropsch (FT) biodiesel produced from black liquor, production costs range from 11.7 and 56.4 €/GJ (13.3–64.2 \$/GJ) (Hansson et al., 2024). To standardise the analysis, an intermediate value of \$1500 was assumed, and \$1000/MT when demand is low and \$2000/MT under the high demand scenario.
- **E-fuels**: The levelized cost of solar electricity is \$0.044/kWh, as reported by IRENE (Jowett, 2024). The cost for hydrogen produced from low carbon electricity ranges between \$3.2 to \$7.7/kg, with \$5/kg adopted in this study (IEA, 2020). The levelized cost for renewable ammonia is reported to range between \$720-\$1400/MT and is projected to fall to \$310–610/MT by 2050, an intermediate value of \$900/MT was used (IRENE and Association, 2022). The renewable methanol reported costs range from \$800-\$1600/MT, projected to fall to \$250–630/MT by 2050, \$1000/MT was used as

the intermediate value (International Renewable Energy Agency; Methanol Institute, 2021).

2.4.4. Overall onboard feasibility assessment

To complement the techno-economic analysis, a qualitative assessment of engine compatibility, required system modifications, regulatory status, technology readiness level (TRL), and integration complexity was conducted for each pathway. The objective was to identify which options are realistically implementable or retrofittable on the reference vessel in the near to medium term, and which remain at a conceptual or developmental stage. The TRL scale follows the standard nine-point definition:

- TRL 1–3: early-stage research and development,
- TRL 4–6: pilot or demonstration level,
- TRL 7–9: commercially available or in widespread use.

3. Results and discussion

3.1. Conceptual design of ship retrofitted for alternative fuels and CCS

When powered by HFO and MDO, the reference ship consumed **204 million MJ** of energy per annum, with a total fuel consumption of 4928 tons, which resulted in CO_2 emissions of **15,526 tons** to deliver 99 million MJ of power output, achieving an overall energy efficiency of **48.5%** using the current 2-stroke engine for propulsion and the current diesel engines for electricity generation. The low carbon ship was designed to deliver the same amount of energy output as the reference ship. The conversion efficiency of CCGT, hydrogen fuel cell, and electrical motor is assumed at 51.6% (Law et al., 2024), 60% (Law et al., 2021) and 92.5% (Law et al., 2021). The vessel is designed with containment capacity to deliver 24.25 million MJ of output. With this, a system powered by CCGT, fuel cell and electrical motor were designed to hold approximately 47.0, 40.4 and 26.2 million MJ of energy source.

3.1.1. Conceptual design of amine-based post-combustion CCS

Using LNG as fuel, the amine-based Post-CCS system achieved a reboiler duty of 3850 kJ/kgCO_2 at 90% capture efficiency, aligning with literature values (Øi, 2007; Arachchige et al., 2019; Du et al., 2021). Under turndown conditions as outcome from hydraulic checks, the duty increased to 6100 kJ/kgCO_2 due to higher steam requirements to maintain stable column hydraulics and avoid convergence issues in the simulation. The system was set to operate above 30% design capacity, achieving a gross CO_2 capture rate of 62%, which translates to a net reduction of 47% after accounting for the 39.75% fuel penalty.

Compared to HFO(CCS), LNG(CCS) achieved a higher net CO_2 emission reduction but with a higher fuel consumption increase. The performance of both post-combustion CCS systems is summarised in Table 5. Over the design voyage, 827–1840 tons CO_2 were estimated to be captured for HFO(CCS) and LNG(CCS), respectively, requiring 2–4 storage tanks of size 450 m^3. The CAPEX of the system was estimated at \$10.7-\$17.3 M. The CO_2 avoidance cost range from \$98- \$242/ton CO_2. Tank and plant layout (Fig. 13) shows the integration at the aft without cargo space loss.

3.1.2. Conceptual design of SMR-H2 plant for pre-combustion carbon capture

Two SMR-H2(CCS) systems, one firing methane and the other one firing reformate to generate reforming heat (denoted as SMR-H2(CCS)* and SMR-H2(CCS)), are discussed here. As shown in Table 5, the SMR system firing reformate achieved a higher net capture efficiency at a higher fuel penalty. In comparison to PostCCS, the SMR systems captured significantly more CO_2, requiring 5–8 tanks for storage of captured CO_2. The CAPEX of the system was estimated at \$43.2M-\$52.8 M (International Energy Agency IEA, 2017; Law et al., 2023b), resulted in a CO_2 avoidance cost range from \$166-\$169/ton CO_2. By

Table 5
Key performance parameters of different OCCS system configurations.

Parameters	HFO(CSS) in Ref (GCMD; Stena Bulk; OGC, 2024).	LNG (CCS)	SMR-H2 (CCS)* SMR in Ref (Law et al., 2024).	SMR-H2(CCS) (Improved from Ref (Law et al., 2024).)
Primary fuel	HFO	LNG	LNG	LNG
SMR furnace fuel	-	-	LNG	Reformate
Reboiler fuel	HFO	LNG	N/A	N/A
Net CO_2 capture rate (%)	19.7%	47%	61.33%	82.82%
Fuel penalty (%)	9.2%	39.8%	24.46%	63.93%
Design capacity:				
Fuel storage capacity (m^3)	1390	3326	2783	3666
CO_2 captured (tons)	827	1840	2009	3574
CO_2 storage volume (m^3)	802	1785	1949	3466
CAPEX (M\$)	\$10.73	\$17.34	\$43.21	\$52.76
ACAPEX (M \$/year)	\$0.43	\$0.69	\$1.73	\$2.11
CO_2 avoidance cost (\$/ton CO_2)	\$242.20	\$98.22	\$166.88	\$168.81
Per annum:				
CO_2 emitted (tonCO_2/year)	13,754	8466	5169	3025
CO_2 avoided (tonCO_2/year)	1772	7060	10,357	12,501
CO_2 reduction rate (% as compared to reference ship)	11%	45%	67%	81%
H_2 production cost (\$/kgH_2)			\$0.89	\$0.66

assuming a theoretical production rate of 1 kg H_2 for every 2 kg of LNG, the production cost of 1 kg of hydrogen was estimated to be equal to \$0.66–0.89/kgH_2, which is higher than the production cost reported by IEA of \$0.61/kg H_2 for hydrogen plant with CCUS (IEA, 2019), but reasonable for a smaller scale of production plant.

As compared to the reference ship without OCCS with 15,526 tons CO_2 emissions, 10,357–12,501 tons of CO_2 was avoided (67–81% reduction rate). This is higher than post-combustion CCS which achieved 11–45% of CO_2 reduction rate when comparing with the reference ship. The usage of LNG as the source of energy significantly reduces the CO_2 intensity. Additionally, the CCGT system improved energy conversion efficiency also reduces fuel consumption. However, LNG fuel tanks are needed for this concept. Due to the excessive space needed for CO_2 storage, the remaining tank space is not sufficient for LNG fuel and additional fuel tanks must be added below deck. As the SMR concept is electrical propelled, replacement of 2-stroke engine with CCGT propulsion system provided flexibility to utilise the space in the engine and machinery rooms. Hence, the conceptual plant layout for SMR-H2(CCS) is shown in Fig. 14. As compared to the post-CCS system, the SMR-H2 plant does not involve tall columns such as absorber and regenerator, however, the size of reformer unit would be quite bulky and requires large footprint. Given the reserved volume as indicated, the Pre-CCS should fit well and no cargo space loss is anticipated.

3.1.3. Conceptual design of electrically propelled bulk carrier

When the reference ship is converted to electric propulsion, a battery storage system with total capacity of 26.2 million MJ must be installed to supply the required electrical energy. Using the specifications of a Tesla Megapack (battery density of 1989 kg/m^3 and energy density of 1224 kJ/kg), each unit equivalent to size of a standard container, approximately 283 container-sized battery units were required. As shown in Fig. 15, a total of 288 container-sized battery units were

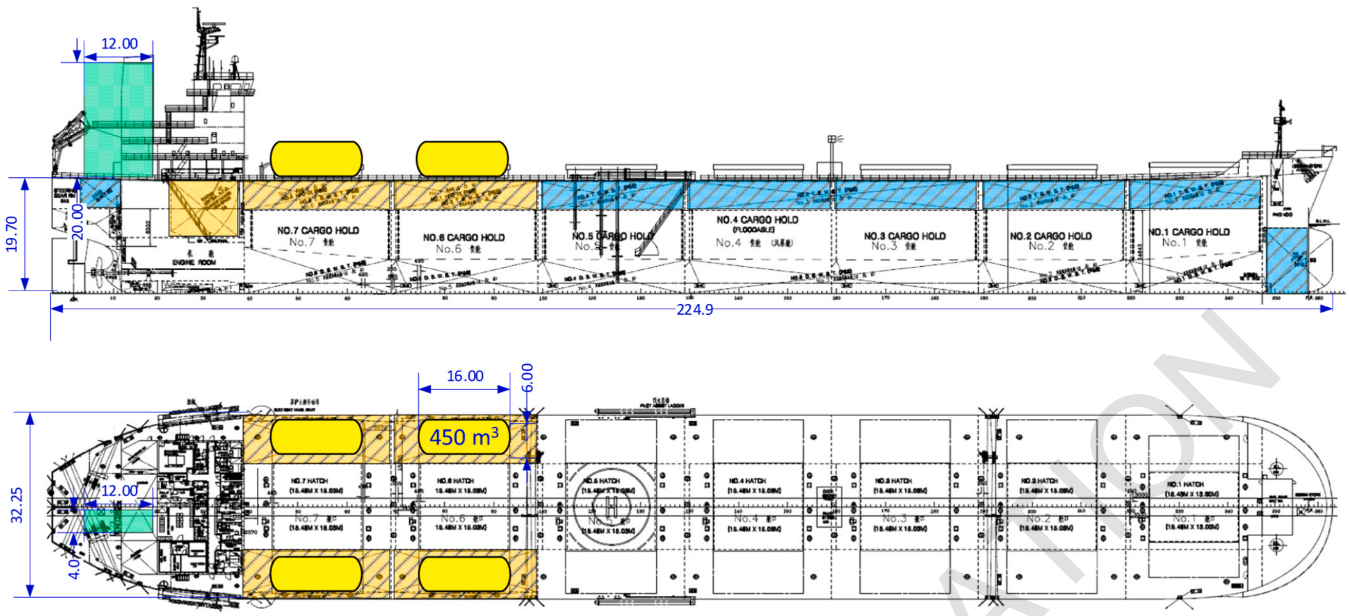

Fig. 13. The general arrangement for the reference ship fuelled by HFO retrofitted with a post-combustion carbon capture system (OCCS). The shaded areas represent the existing fuel tanks, while the yellow cylindrical tanks (approximately 450 m^3 each; radius 3 m, length 16 m) indicate the proposed installation of Type C storage tanks for captured CO_2. These tanks are arranged symmetrically along the port and starboard sides near the cargo hatch region to optimise space utilisation. The green-shaded volume at the aft section represents the reserved volume of 960 m^3 for placement of OCCS plant. Based on this conceptual layout, cargo space sacrifice was avoided.

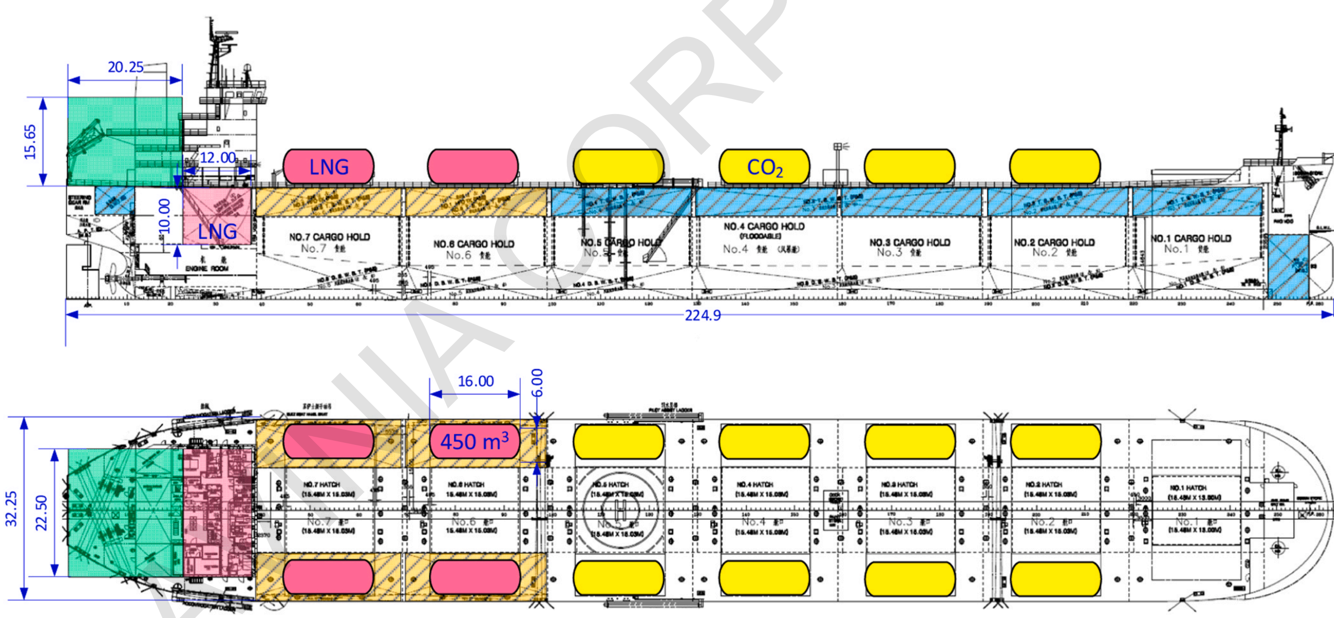

Fig. 14. The general arrangement for the reference ship retrofitted with onboard hydrogen production and pre-combustion carbon capture system (PreCCS). A total of 12 Type C cylindrical storage tanks (approximately 450 m^3 each; radius 3 m, length 16 m) are installed symmetrically along the port and starboard sides. These include 4 tanks for storage of LNG fuel and 8 tanks for captured CO_2. The red-shaded volume represents the reserved space for the LNG storage tank (approximately 2700 m^3), while the green-shaded volume indicates the allocated space for the PreCCS plant. The layout utilises available deck space and aft sections to accommodate additional equipment, enabling system integration without compromising cargo hold capacity.

arranged on the deck and at the aft side of the ship, occupying 10,962 m^3 of free space.

The battery system would add approximately 21,418 tonnes of weight, equivalent to ~30% of the vessel's cargo capacity, resulting in a potential 30% reduction in cargo-carrying capability. In addition to the significant space and weight penalties, the annualised CAPEX (ACAPEX) of the battery system is considerably higher than that of conventional propulsion and alternative low-carbon systems. Consequently, full battery-electric propulsion is not a technically or economically viable option for this vessel, particularly for long-range voyages.

3.1.4. Containment system requirements

Table 6 summarises the additional space and deadweight requirements for each fuel type. Among the liquid fuels, biodiesel can be

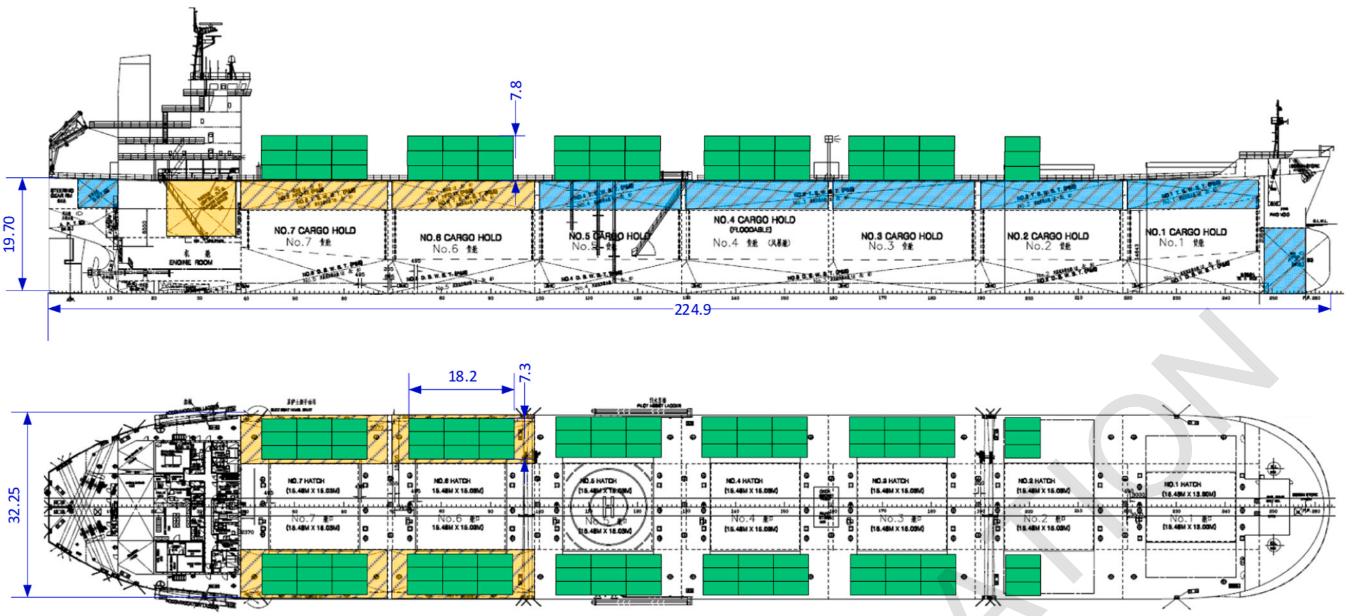

Fig. 15. The general arrangement for the reference ship retrofitted with battery system, a total of 288 container-sized battery units were arranged on the deck and at the aft side of the ship to provide storage for 26.2 million MJ of electricity.

Table 6
Estimated added mass, added volume and annualised CAPEX of various fuel storage system. The relative mass and volume are estimated in relative to the mass and volume of HFO. For CCS pathways, the added mass and volume of captured CO_2, and the relative mass and volume including captured CO_2 are shown in parentheses.

Pathways	Fuel mass, m_{fuel} (tons)	[1]Fuel volume, V_{fuel} (m^3)	Relative mass	Relative volume	[2]Added fuel deadweight (tons)	[3]Added fuel volume (m^3)	ACAPEX ($/year)	Relative ACAPEX
HFO	1235	1340	1.00	1.00	0	0	60,200	1
LNG	1018	2505	0.82	1.87	0	2120	240,770	4
H_2	417	5848	0.34	4.37	0	5463	481,541	8
NH_3	2688	4764	2.18	3.56	288	4379	150,482	2.5
MEOH	2513	3339	2.04	2.49	113	889	80,257	1.3
Electricity	21,418	10,768	17.35	8.46	19,018	10,768	389,245,586	6484
Biodiesel	1163	1407	0.94	1.05	0	0	60,200	1
HFO (CCS)	1348 (+827)	1390 (+802)	1.09 (1.76)	1.04 (1.64)	0	802	66,268	1.1
LNG (CCS)	1424 (+1840)	3326 (+1785)	1.15 (2.64)	2.48 (3.81)	0	4726	336,358	5.6
SMR-H2 (CCS)*	1191 (+2009)	2783 (+1949)	0.96 (2.59)	2.08 (3.53)	0	4347	281,654	4.7
SMR-H2 (CCS)	1569 (+3574)	3666 (+3466)	1.27 (4.16)	4.19 (5.32)	1174	6747	370,990	6.2

Note: 1. Storage tank is 95% filled. 2. Considering the fuel deadweight of the reference vessel (2400 tons), the additional fuel deadweight is calculated as the difference between the alternative fuel deadweight and that of the reference ship. For alternatives requiring less than 2400 tons, the added deadweight is zero. For CCS options, the fuel mass is taken as either the deadweight of the captured CO_2 or the fuel deadweight, whichever is larger. Similarly, if this value is less than 2400 tons, it is treated as zero added deadweight. 3. Considering the total capacity of fuel oil tanks of 2450 m^3, biodiesel and methanol can be stored in the same tanks with minor retrofit, whereas other alternative fuels can utilise the aft tank of 385 m^3; therefore, the added fuel volume is the difference between the usable tank space and the total fuel volume required by the alternative fuels.

stored entirely within the existing fuel tanks, requiring no additional storage space. Methanol can also utilise the existing tanks but, due to its lower energy density, an additional ~900 m^3 of storage capacity is required. As methanol does not require specialised tanks, the additional volume can be accommodated in the aft zone of the vessel without major structural modifications.

In contrast, cryogenic fuels (LNG, H_2, NH_3) require Type C tanks with specialised insulation to limit boil-off rates to below 1.5% per day. Only a small portion of the existing fuel space near the engine room (385 m^3) is assumed utilised. The number of tanks required for LNG, H_2, and NH_3 were 5, 12 and 10, respectively. The tanks should be distributed equally across the port and starboard zones for optimal stability. These tanks were distributed symmetrically along the port and starboard sides to maintain vessel stability. The maximum number of tanks that can be accommodated on deck is 14, allowing all cryogenic alternatives to be integrated without affecting the cargo space (Fig. 4).

The CAPEX of the storage system depends primarily on the number of tanks, tank material, and insulation requirements. Using cost factors from (Law et al., 2021). the annualised CAPEX over a 25-year operational life was estimated and summarised in Table 6. Among the alternatives, electricity storage systems were the most expensive, followed by H_2, LNG, NH_3, MeOH and lastly biodiesel, which was comparable to conventional fuel storage costs.

3.2. Alternative options comparison

This section compares six alternative fuels (LNG, H_2, NH_3, MeOH, Electricity, biodiesel) and OCCS across technical, environmental, and economic dimensions. From conceptual design, the added mass and volume of the alternative systems were estimated and summarised in Table 6.

3.2.1. Technical: space and stability

Space (volume): As illustrated in Fig. 4, Fig. 13, Fig. 14, retrofit integration of most alternatives can be achieved by utilising space above the deck, avoiding intrusion into cargo holds. This enables retention of the cargo capacity.

Stability (deadweight and COG): The added deadweight associated with most alternative fuel systems is modest (< 1.6% of the vessel's original weight) and does not significantly affect stability, expect for electricity alternative which added 30% weight to the reference ship, which would potentially reduce cargo deadweight allowance and directly impacts on the operating economics. When heavy equipment is concentrated in the aft zone, the centre of gravity and metacentric height change, necessitating a stability reassessment and potential reclassification of the vessel. Structural verification would also be required if additional weight exceeds the vessel's design limits.

3.2.2. Technical: safety

For HFO, biodiesel and LNG, safety regulations have been established for offshore applications. Therefore, vessel modifications to accommodate these fuels can follow existing regulatory frameworks. In contrast, hydrogen, ammonia, and methanol introduce new hazards, requiring enhanced safety measures and careful system integration. In general, fuel tanks must not be located in machinery spaces or accommodation areas and must be protected from mechanical damage to prevent leaks. Piping traversing accommodation spaces should employ double-wall designs, and gas detection, automatic shutdown, and ventilation systems are essential in confined spaces. Table 7 summarises the flammability, toxicity, corrosiveness, explosion risk, and handling complexity of the various fuels and CO_2 storage systems, providing a basis for safety considerations in design.

H_2 has a wide flammability range (4–75% in air) and explosive risk should include Tank Connection Spaces (TCS) and secondary enclosures under vacuum to prevent gas accumulation and ignition (European Maritime Safety Agency EMSA, 2024a). NH_3 as a highly toxic and corrosive fuel could cause health risks at concentrations as low as 25–50 ppm, with fatal exposure possible at 300 ppm. Classification societies generally limit ammonia release to 25–30 ppm, with gas detectors triggering shutdowns at 150–300 ppm. Interim guidelines specify safety distances of 10–25 m between ammonia vent outlets and accommodation air intakes (European Maritime Safety Agency EMSA, 2024b). Methanol as another high flash point fuel must incorporate the same safety features required for ammonia and hydrogen, including proper containment, leak detection, and emergency shutdown mechanisms (Arian et al., 2018).

3.2.3. Environmental: CII, IMO EFI and Fuel EU Maritime regulations

Table 8 summarises the WTT and TTW emissions, CII, and GHGIE or GFI of the various pathways. By comparing the WTT emissions factors, fossil-based fuels (BLUE pathways) such as blue H_2 and NH_3 which have zero TTW emissions, emit significantly higher emissions during fuel production stage, resulting in overall GHGIE values higher than conventional fuels. For blue MeOH, both TTW and WTT emissions contribute to higher total GHGIE. Blue fuels produced from fossil electricity are particularly carbon-intensive due to losses during electricity generation and the energy-intensive nature of their respective production processes. Consequently, all blue pathways were excluded from further analysis, as they do not deliver meaningful emission reductions. Similarly, LNG with a GHGIE of 83.83gCO_{2eq}/MJ, can only meet the emission compliance until 2030. Consequently, it should not be considered a sustainable long-term solution.

For biofuels, when TTW CO_2 emissions are assumed offset by atmospheric CO_2 absorbed during biomass growth, the TTW CO_2 emissions are considered negligible. Then, the GHGIE of biofuels is primarily determined by their GHG_{WTT} values. Fig. 16 illustrates the WTT emissions of various biofuel pathways, ranging from 2.2 to 75.7 gCO_{2eq}/MJ, depending on emissions during biomass cultivation (e_{ec}), processing and production methods (e_p) and transportation (e_{td}) taken from EU Directive 2018/2001 (European Union, 2018). The summation of e_{ec}, e_p and e_{td} gives GHG_{WTT}. The pathway descriptions and a detailed breakdown of the WTT emissions are provided in the Appendix A (Table B2). The

Table 7
Flammability, toxicity, explosivity and complexity of selected fuels and CO_2. Colour coding is used to indicate the level of hazard or complexity: green = low, yellow = moderate, and red = high (DMA, 2007; Fan et al., 2024; U.S. Department of Energy, 2025; ABS, 2019).

Pathways	*Flammability*	*Toxicity*	*Corrosiveness*	*Explosion risk*	*Handling complexity*
HFO	Moderate (flash point ≥ 60 °C) [81]	Moderate toxicity (chronic concern)	Low–Moderate (sulphur content)	Low	Low-Moderate
LNG	Moderate (LFL–UFL ≈ 5–15% in air) [82]	Low (asphyxiant)	Low	High-Moderate	High (cryogenic, insulation, boil-off)
H_2	Very High (LFL–UFL ≈ 4–75%; invisible flame) [82]	Low (asphyxiant)	Moderate (embrittlement of some metals)	Very High	Very High (cryogenic, leak risk)
NH_3	Moderate (LFL–UFL ≈ 15–28% in air) [82]	Highly toxic	High	Moderate-Low	High (cryogenic, toxic handling + material sensitivity)
MEOH	High (flash point 11°C) [56]	High systemic toxicity	Moderate	Moderate	Moderate
Biodiesel	Low (flash point ≥ 93 °C, often ~130 °C) [83]	Low	Low–Moderate (Can oxidize and form acidic products)	Low	Low
CO_2 (Storage)	Non-flammable	Low (asphyxiant)	Low–Moderate (acidic when wet)	Low	High (cryogenic)

Table 8
GHG_{WTT}, GHG_{TTW} and GHGIE for selected marine fuel pathways.

Pathways	GHG_{WTT}(gCO_{2eq}/MJ)	GHG_{TTW} ($gCO_{2e}q$/MJ)	GHGIE, GFI	CII	Potential fuels (Yes/No)
HFO	13.50	78.10	91.60	3.50	No, high GHGIE
LNG	18.50	65.33	83.83	2.55	No, high GHGIE
Blue H2	132.00	0	132.00	0	No, high GHGIE
Blue NH3	121.00	0	121.00	0	No, high GHGIE
Blue MEOH	31.30	69.10	100.40	3.15	No, high GHGIE
Blue E	27.78	0	27.78	0	No, low CAR
Blue E-H2	132.00	0	132.00	0	No, high GHGIE
Blue E-NH3	121.00	0	121.00	0	No, high GHGIE
Blue E-MEOH	31.30	69.10	100.40	3.15	No, high GHGIE
Biodiesel (Soybean)	47.00	0	47.00	0	Yes
Biodiesel (black liquor)	10.20	0	10.20	0	Yes
Solar E	19.17	0	19.17	0	No, low CAR
Solar E-H2	31.82	0	31.82	0	Yes
Solar E-NH3	37.63	0	37.63	0	Yes
Solar E-MEOH	37.90	0	37.90	0	Yes
HFO (CCS)	13.50	62.95	76.45	3.07	Yes
LNG (CCS)	18.50	39.46	57.96	1.89	Yes
SMR-H2 (CCS)*	18.50	22.25	40.75	1.16	Yes
SMR-H2 (CCS)	18.50	10.22	28.72	0.68	Yes

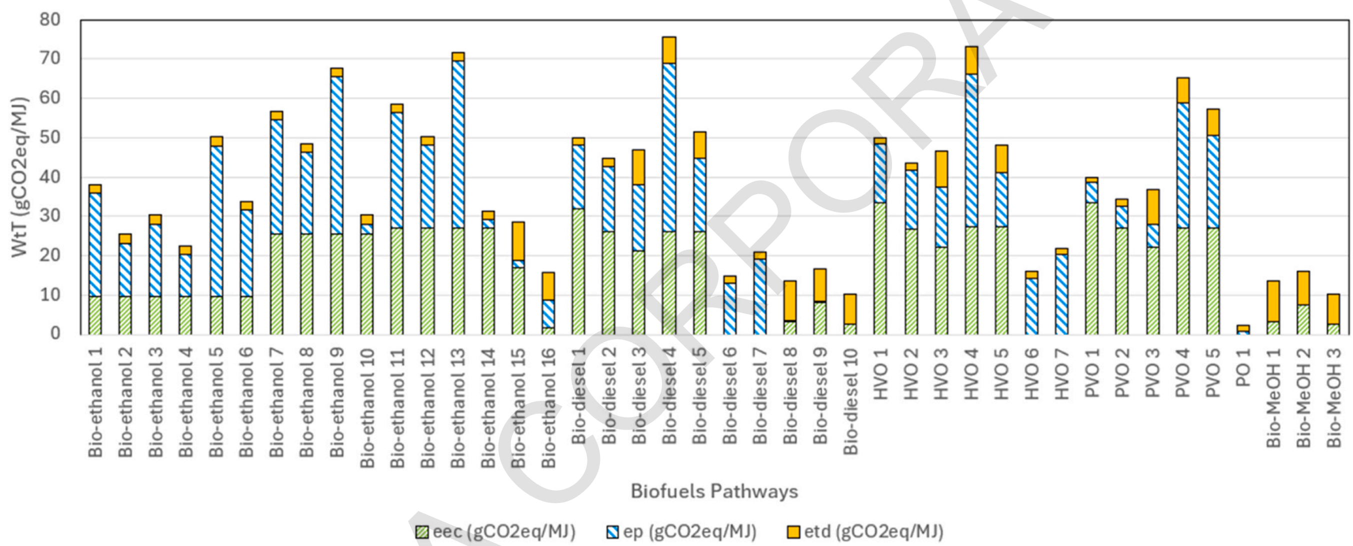

Fig. 16. Well-to-tank emissions factors (WTT gCO_{2eq}/MJ) for biofuels produced from different pathways with the description of the pathways included in Appendices A (Table B2). The emission factors: biomass cultivation (e_{ec}), processing and production methods (e_p) and transportation (e_{td}) taken from EU Directive 2018/2001 (European Union, 2018), and the summation of e_{ec}, e_p and e_{td} gives GHG_{WTT}.

biofuel pathway with the lowest WTT emissions is PO 1, produced from waste cooking oil. Other biofuels such as biodiesel, hydrotreated vegetable oil (HVO), and bio-methanol also exhibit relatively low WTT emissions, typically in the range of 10–20 gCO_{2eq}/MJ. In this study, two representative biofuel pathways were selected for further assessment:

- High WTT: Soybean biodiesel (47 gCO_{2eq}/MJ)
- Low WTT: Fischer–Tropsch biodiesel from black liquor gasification (10.2gCO_{2eq}/MJ)

Green fuels are also assumed to have zero TTW emissions. Therefore, their total emissions are dominated by emissions during fuel production stages. Solar electricity generated from photovoltaics (PV) systems has estimated lifecycle emissions of 45–69 gCO_2/kWh (National Renewable Energy Laboratory, 2012; Mehedi et al., 2022; Nugent and Sovacool, 2014). In this study, 69 gCO_{2eq}/kWh (19.17 gCO_{2eq}/MJ) is used in estimation of lifecycle emissions of other fuels produced from solar electricity. By using the WTT energy factor expressed as the amount of energy consumed per MJ of fuel produced in preliminary work published in (Law et al., 2021), (0.66, 0.963 and 0.977 for Solar-E-H_2, Solar-E-NH_3 and Solar-E-MeOH, respectively), the resulting WTT emissions are approximately 31.82, 37.63 and 37.90 gCO_{2eq}/MJ for Solar-E-H_2, Solar-E-NH_3 and Solar-E-MeOH.

For fossil fuels, integrating CCS provides a viable pathway to reduce lifecycle emissions, provided that the captured CO_2 is permanently stored. In this study, the CCS pathways lowered the GHGIE to 28.8 – 76.5 gCO_{2eq}/MJ, with pre-combustion technologies achieving greater reductions than post-combustion systems. Such reductions could extend the regulatory compliance period of fossil fuels, positioning CCS as a transitional decarbonisation strategy for the maritime sector.

3.2.4. *Economics: fuel cost, cargo space loss, carbon tax*

Fuel cost constitutes a significant portion of a vessel's OPEX, which is why high fuel prices remain a major barrier to the adoption of green hydrogen and ammonia (Korberg et al., 2021; Kanchiralla et al., 2023). As shown in Fig. 17, the unit cost of the fuel could affect the operating cost by millions of dollars. For instance, when biodiesel is priced at \$1000/MT under a low demand scenario, the annual OPEX for the reference ship was \$4.7 million. However, this cost could double to \$9.5 million per year when biodiesel demand is higher or when the biomass

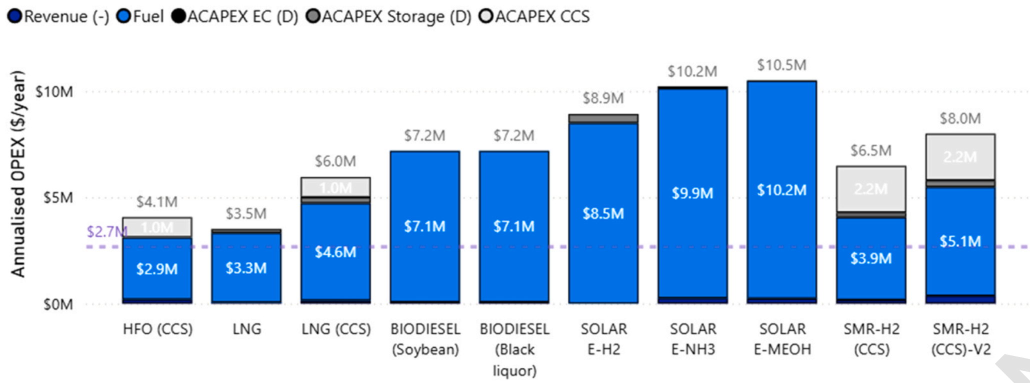

Fig. 17. Economic projection of selected low carbon alternatives.

feedstock becomes more expensive due to competition with food production. A similar trend may occur with green fuels, which are currently limited by low production rates. Nevertheless, ongoing technological advancements are expected to reduce the cost of green fuels in the near future.

Different from biofuels and green fuels, the fossil-fuels options have a much lower annual fuel cost in the range of $2.7 - $3.3 M/year without CCS, increasing to $2.8 - $5.1 M/year with CCS integration due to fuel penalty of CCS operation. Although the OPEX for CCS options are relatively low, CAPEX investment for the new technology and storage system result in higher overall expenses between $4-$8.1 M/year. This price could potentially reduce when the technologies become more developed.

The difference in the CAPEX for the fuel containment system was not significant when amortized over a 25-year payback period, except for the electrification pathway with an annualised cost of $389 M/year due to the battery cost. Excluding the electrical pathway, the cost of fuel containment system is highest for H_2, followed by LNG, NH_3, MeOH, and diesel fuels. When the same alternative fuel combined with different propulsion systems is considered, adoption of fuel cells led to a substantial cost increment of approximately $4 million per year, as compared to the conventional pathways. This is due to the current market price for fuel cells being 11.5 times higher than that of ICE (Law et al., 2021), which outweighs any potential fuel cost savings from their improved efficiency. This finding is consistent with findings in (Kanchiralla et al., 2023) and (Korberg et al., 2021). Therefore, fuel cell pathways were excluded from further consideration in this study until the technology becomes cost-competitive with combustion engines.

Lastly, emission penalties must also be considered when evaluating the economics of low-carbon solutions compared to conventional ships, as these penalties can significantly increase the OPEX for high-emission pathways. From Fig. 18, when emission caused by 50% of the energy used is taxed under Fuel EU and subjected to purchase of EUA which is assumed traded at $100/ton of CO_2, and the remaining 50% under IMO GFI, the cost of penalties is projected to rise in line with increasingly stringent regulatory reduction targets from $0.9 to $9.3 M/year by 2050.

3.2.5. Overall onboard feasibility assessment

The retrofit feasibility varies significantly across pathways, largely depending on engine compatibility and regulatory maturity. Table 9 summarises the engine compatibility, required system changes, regulatory status, TRL, and integration complexity for the evaluated low-carbon pathways. In general, the introduction of two-stroke gas engines capable of operating on hydrogen, ammonia, and methanol can reduce the scale of required modifications, as these engines are designed for relatively straightforward retrofits (MAN Energy Solutions, 2024). In contrast, electricity-based and SMR-CCS pathways require complete powertrain replacement, while LNG and CCS retrofits involve extensive modifications to fuel systems and ship layout. Biodiesel pathways are the least complex, requiring only minor system cleaning and adjustments, making them the most immediately deployable option.

- **Biodiesel and methanol** are the most mature options, with high TRLs (7–9), existing regulatory approval, and minimal or moderate

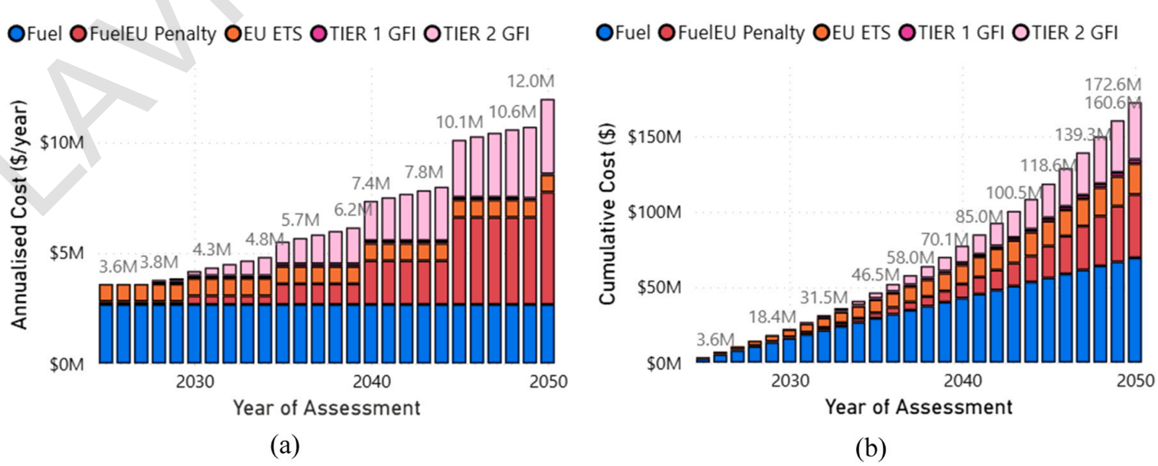

Fig. 18. Economic projections for the reference ship under the implementation of Fuel EU, EU ETS and IMO GFI penalty systems: (a) annualised cost, (b) cumulative cost.

Table 9
Engine compatibility required system changes, regulatory status, the technology readiness level, and integration complexity for the selected low-carbon pathways. Colour coding indicates relative implementation difficulty, where green = low, yellow = moderate, and red = high (MAN Energy Solutions, 2024; Habibic, 2025).

Pathways	Engine compatibility	Required system changes	Regulatory approval status	TRL	Integration complexity
H_2	Engine replacement likely, 2-stroke ME-GI gas engine has been tested on H_2 [88].	New engine, add Type C fuel tanks, new double-walled piping system, add safety and ventilation systems.	No finalised IMO Code, approval is case-specific with risk assessment	4-6	High
NH_3	Engine replacement likely, 2-stroke ME-LGI-Ammonia has been tested on 100% load [89].	New engine, add Type C fuel tanks, new double-walled piping system (or ventilated secondary enclosure), add safety and ventilation systems, add gas detection system, add scrubbers for NO_X	No finalised IMO Code, approval is case-specific with risk assessment	4-6	High
MEOH	Engine replacement likely, 2-stroke ME-LGI-Methanol has been tested on 100% load [89].	Tank retrofit (coating), add additional Type C tank, add safety and ventilation systems,	Approved, IMO Interim Guidelines	7-9	Medium
Electricity	Engine changed to e-propulsion.	Battery installation, new powertrain, excessive weight added	Approved.	7-9	High
Biodiesel	Compatible for biodiesel blends (B20, B30). B100 lacking for continuous commercial operation.	Minor changes, cleaning may be required.	Approved, no additional IMO code required.	7-9	Low
HFO (CCS)	Compatible, no change to engine.	add Type C fuel tanks, major layout changes	HFO approved, CCS received AiP from classification	7-9	Medium
LNG (CCS)	Retrofit to dual-fuel LNG (ME-GI or LGI) required.	add Type C fuel tanks, new double-walled piping system, safety systems, major layout changes	LNG fully approved; CCS received AiP from classification	7-9	High
SMR-H2 (CCS)	This pathway assumed replacement with CCGT + electric propulsion.	New CCGT, new powertrain, add Type C fuel tanks, major layout changes	LNG fully approved; CCS is a new concept	7–9 (land)	High

retrofit requirements, making them the most straightforward for near-term implementation.

- **LNG and post-combustion CCS** systems are also at high TRL, with classification society approval in place; however, they involve significant system modifications such as Type C tank installation, double-walled piping, and safety systems, leading to medium-to-high retrofit complexity.
- **Hydrogen and ammonia** retrofits remain technically challenging, requiring engine replacement, additional safety measures, and operating under case-by-case approval due to the absence of finalised IMO codes. Their TRLs are currently in the mid-range (4–6).
- **Electric propulsion** has a high TRL but is more suitable for short-sea shipping rather than deep-sea operations.
- **SMR-CCS pathways** demand complete powertrain replacement and major layout modifications, representing the highest retrofit complexity. However, the SMR technologies have high TRL for land-based applications.

Overall, Table 9 highlights that while several pathways are technically and economically feasible, only a subset particularly biodiesel, methanol are sufficiently mature and less complex for near-term retrofitting. Nevertheless, case-specific approvals and tailored system designs can enable the adoption of other pathways, provided that supply chain issues are addressed.

3.3. Discussion

This study developed a low-carbon ship design by integrating historical voyage and ship data with physics-based models for alternative fuels and OCCS. This framework allows ships powered by low-carbon alternatives to be optimally designed to meet voyage requirements while avoiding overdesign. Historical voyage data were analysed to characterise the reference ship's operational profile (Fig. 6), fuel consumption (Fig. 7) and emissions (Fig. 8) patterns. It was found that the fuel consumed between bunker calls ranged between 13.2 and 77 million MJ, with the upper end corresponding to a 4-month voyage. To ensure practicality, the fuel containment capacity was set at 50 million MJ, based on opportunities for intermediate bunkering. This demonstrates how operational data can inform realistic and cost-effective design decisions.

The OCCS was designed and hydraulically verified in Aspen HYSYS, revealing wide variation in amine regeneration duty under turndown conditions, with energy penalties increasing significantly at low loads. Pre-combustion SMR-H_2 in (Law et al., 2024) after modifying to fire reformate for heat generation, achieved a maximum net capture rate of 82.8%, reducing emission intensities of the ship to 28.72gCO_2eq/MJ and CII to 0.68 gCO_2/dwt.nm. In comparison, post-combustion systems were limited by their minimum turndown (30% load), resulting in lower overall reduction. In addition, the LNG(CCS) pathway showed the highest fuel penalty among all configurations (~0.22 kgCO_2 consumed per kg CO_2 captured), followed by the modified SMR, HFO(CCS), and lastly the base SMR (Law et al., 2024). CO_2 avoidance ranged between $98-$242/ton CO_2 reduced, highest for HFO(CCS) due to low capture efficiency. Overall, pre-combustion CCS provided the best capture performance.

The existing tanks were re-used whenever possible, while cryogenic fuels were stored using standard 450 m^3 Type C tanks. Free deck space on the port, starboard, and aft zones were allocated to accommodate fuel tanks, CO_2 capture tanks and the CCS module. Most concepts could be retrofitted without impacting cargo capacity, though weight increases required stability checks. In this study, it was assumed that added equipment weight offset an equivalent reduction in cargo deadweight, maintaining vessel stability. Among the fuel options, electricity-based systems added the most weight (30% of cargo deadweight), making them impractical for long-haul operations, whereas the other alternatives with cargo loss of below 1.6% had minimal impact on vessel performance

Technical assessment of the selected alternatives considered the space, stability and safety aspects. As discussed, added volume was minimised through efficient use of free space. Weight was evenly distributed to reduce impact on the center of gravity, thus avoiding further stability checks. Safety assessment emphasized the needs of integrating additional safety features for safe operation. The fuel containment system must be protected against mechanical damage to mitigate any potential leakage, the piping system must be designed with second enclosures such as double wall design to vent leaks safely, safety distance from accommodation zones of 20 m is needed, and safety features such as gas detectors, automatic shutdown systems, and ventilation is needed in confined spaces.

From an environmental standpoint, ideal low-carbon fuels are those with low GHGIE and GFI values. Notably, a low CII score does not guarantee low lifecycle emissions. This was evident with blue fuels, which, despite low operational emissions, exhibited high WTT emissions, making them less sustainable than their green counterparts. Consequently, all blue fuel options were excluded from further assessment. LNG was also excluded as a long-term solution, as it only meets emissions compliance up to 2030. Regarding biofuels, although their TTW emissions are assumed negligible, the European Council reports the GHG_{WTT} of biofuels ranging between 2.2 and 75.7 gCO_{2eq}/MJ depending on feedstock cultivation, processing, and transport (European Union, 2018). According to the IPCC and IMO GHG Study, indirect land-use change (ILUC) can further increase these values, in some cases offsetting decarbonisation benefits (Ricardo, 2024). Bio-methane, with reported lifecycle emissions from −85.5–41 gCO_{2eq}/MJ is another promising option (Majer et al., 2016). In short, biofuels produced from sustainable feedstocks and with low WTT emissions are the preferred choice. For all fossil-based fuels, carbon capture could potentially lead the way to low emissions, but this would only be recognised with the CO_2 captured can being permanently stored. In the two OCCS pathways that were included in this study, Pre-combustion CCS has potential to drive the Fuel EU compliance until 2049, while LNG(CCS) until 2044, and HFO(CCS) is compliant until 2039. This demonstrates the value of CCS in long-term maritime decarbonisation.

From an economics aspect, fuel cost is a significant contributor to the total operating expenses. The reference ship recorded an annual OPEX of $2.7 M/year, which was projected to triple with green fuels to $8.5 - $10.2 million/year. Based on historical trend of the green fuel's prices, green fuels could potentially become cheaper. With biodiesel, the fuel cost was projected to increase by approximately $2 million/year even when biodiesel was priced at $1000/MT. However, the supply of biofuels is constrained by competition for land and water with the food industry; hence, the price of biodiesel could become higher (approaching $2000/MT). The study also revealed that the OPEX for the OCCS options remain competitive due to stable fossil fuel prices. Based on projections of available oil and gas reserves, their abundance could help keep fuel prices relatively stable. However, governments may intervene by taxing fossil fuels in the future. Therefore, there are various possibilities in the future market which could affect the economics of various alternative pathways.

Apart from OPEX, CAPEX is equally important, especially for pathways that require changes to the fuel containment system and with additional equipment. The ACAPEX for the containment system was found to be affordable, expect for the electricity-based option with high battery price. For OCCS, the possibility to reduce the ACAPEX for CCS technologies could make them a more attractive pathway. In addition, some fuels can consider using energy converters such as fuel cell with higher energy conversion efficiency, if the CAPEX for fuel cell is becoming cost-competitive with combustion engines. This study concluded that decarbonisation is always accompanied with a significant cost, either additional CAPEX or higher OPEX or both. Therefore, the imposition of carbon taxes and penalties on emissions with incentives for reductions can help incentivise the transition. In summary, the economic uptake of low-carbon alternatives is highly dependent on fuel price fluctuations, supply chain development, and regulatory control mechanisms. In addition to market volatility, technological development will affect the CAPEX of battery and fuel cell technologies, which could significantly impact the feasibility of these advanced alternatives.

Finally, it is important to note that the quantitative findings reported in this study are specific to the reference ship, as projections were based on historical trips and voyages data. However, the same approach could be adapted for other vessels, provided that historical data is available.

Fuel market trends, supply-demand dynamics, and technological advancements will continuously shape feasibility. Alternative fuels such as blue and green hydrogen, ammonia, and methanol remain costly, which require significant scaling to meet global demand. Biofuels, while cheaper, face supply limitations. For CCS, maintaining acceptable CAPEX levels ensure a reasonable payback period, making it more attractive. This assessment ruled out several alternative pathways, including:

- Electricity-based alternatives (Blue E and Solar E) which are not suitable for long-haul voyages due to space constraints for battery storage system
- Blue fuels without CCS (LNG, HFO and MeOH without CCS) which fail to meet emissions compliance and cannot be considered viable long-term solutions.
- Synthetic fuel produced from LNG-electricity (including Blue E-H_2, Blue E-NH_3, and Blue E-MEOH), which are less economically viable than their counterparts produced directly from LNG and renewable energy (Solar).

The alternative pathways selected from this study as potential solutions for the reference bulk carrier are:

- OCCS alternatives: HFO(CCS), LNG(CCS), SMR-H2(CCS)*, SMR-H2 (CCS)
- Green fuels: Solar E-H_2, Solar E-NH_3, Solar E-MeOH
- Biodiesel with low and moderate WTT emissions (10.2–47 gCO_2eq/MJ).

Based on current conditions, CCS and biodiesel appear to be the most viable alternatives for the reference ship.

4. Conclusions

This study presents a data-driven framework for designing low-emission retrofit solutions for a Panamax bulk carrier by integrating historical operational data with physics-based modelling of alternative fuels and onboard carbon capture systems (OCCS). By leveraging real voyage data, the data-driven approach enables realistic system sizing, avoids overdesign, and ensures operational feasibility. The framework accommodates different low-carbon alternatives, each requiring specific design considerations. A comparative assessment of multiple decarbonisation pathways including LNG, H_2, NH_3, methanol, biodiesel, electrical propulsion, and onboard CCS revealed significant variation in performance across technical, environmental, and economic criteria.

From a technical perspective, most alternative fuel and CCS configurations can be integrated within existing vessel layouts by utilising available deck space, with minimal impact on cargo capacity ($<$1.6%). However, electrification pathways impose significant weight penalties ($\sim$30% of deadweight), making them unsuitable for long-haul operations.

From a safety perspective, conventional fuels such as HFO, LNG, and biodiesel can rely on established regulatory frameworks, whereas hydrogen, ammonia, and methanol introduce additional hazards requiring enhanced safety systems, including double-walled piping, gas detection, ventilation, and safe separation distances.

From an environmental perspective, lifecycle emissions analysis revealed that low operational emissions do not necessarily translate to low overall emissions. Blue fuel pathways were excluded due to high upstream emissions, while LNG offers only short-term compliance. In contrast, CCS pathways significantly reduce lifecycle emissions (down to 28.7 gCO_2eq/MJ), with pre-combustion CCS achieving the highest capture performance ($>$80%) and offering extended regulatory compliance potential.

From an economic perspective, fuel cost remains the dominant factor influencing feasibility. Green fuels substantially increase operating costs under current market conditions, whereas CCS pathways remain relatively competitive due to stable fossil fuel prices, despite additional CAPEX and fuel penalties. The overall feasibility is highly sensitive to fuel price evolution, carbon pricing, and policy incentives.

From an overall perspective, CCS-based pathways and biodiesel emerge as the most viable near-term alternatives due to their higher technology readiness and lower retrofit complexity. Green fuels such as hydrogen, ammonia, and methanol could offer strong long-term potential but remain constrained by high costs and limited supply. Ultimately, the feasibility of alternative fuels remains highly dependent on market trends, supply chain development, regulatory frameworks, and financial incentives for low-carbon investments.

Overall, this study highlights the importance of combining real operational data with system-level modelling to support informed decision-making in maritime decarbonisation. The companion Part II paper will extend this analysis through detailed economic modelling and sensitivity analysis to evaluate investment risks and overall CO_2 avoidance costs of selected low-carbon alternatives under evolving market and policy conditions. These findings reinforce that no single pathway is universally optimal, highlighting the need for vessel-specific, data-driven decarbonisation strategies.

CRediT authorship contribution statement

Nikolaos Tsoulakos: Data curation, Conceptualization. **Evita Meristoudi:** Data curation, Conceptualization. **Law Li:** Writing – review & editing, Writing – original draft, Visualization, Validation, Software, Resources, Project administration, Methodology, Investigation, Formal analysis, Data curation, Conceptualization. **Panos Theodossopoulos:** Resources, Data curation, Conceptualization. **Epaminondas Mastorakos:** Writing – review & editing, Supervision, Methodology, Funding acquisition, Conceptualization.

Appendix D the validated aspen model of amine based post-combustion CCS and SMR-PSA pre-combustion CCS

Post-combustion carbon capture system:

Aspen HYSYS process model of the amine-based post-combustion carbon capture (PostCCS) system, adapted from a previously validated steady-state model using blended monoethanolamine (MEA) and methyldiethanolamine (MDEA) as the solvent is shown in Fig. D1 (Law et al., 2017a). The same aspen model was used to simulate the performance of amine-based carbon capture at different loads with varying flue gas flow rate and composition.

As shown in Fig. D1, the flowsheet comprises the key unit operations of an absorber, stripper, lean/rich heat exchanger, reboiler, condenser, and associated pumps and heat integration streams. The flue gas is fed into the absorber column, where CO_2 is chemically absorbed by the amine solution, followed by solvent regeneration in the stripper through thermal desorption. The absorber and stripper columns are modelled as packed columns using BXPLUS structured packing (STANDARD dimension). Column dimensions are determined via hydraulic analysis in Aspen HYSYS to ensure operation below flooding limits under maximum exhaust gas and solvent flow conditions. The model incorporates heat recovery and energy integration to reflect realistic onboard operation. The model is validated against industrial data provided by Tenaga Nasional Berhad Research (TNBR), ensuring reliable prediction of CO_2 capture performance and energy penalty. This model is subsequently used for system sizing and integration within the shipboard carbon capture framework.

The Post-CCS model was firstly sized for the selected capacity. Based on the vessel's operational profile, the selected design capacity is the operation with fuel consumption rate of 948 kg/hr (main engine operational loads of 60%), and exhaust flow rate of 12.14 kg/s. With this, all unit of operation was sized to handle exhaust flow rate of 12.14 kg/s. After equipment sizing, the sized model was used to assess the performance of the post-CCS when engine loads were at 25%, 35%, 50%, and 60%. The flue gas composition at varying engine load was estimated, and the flow rate of MEA/MDEA amine was adjusted in Aspen until absorber and regenerator columns were operated below the flooding and weeping limits. The results from the Aspen simulation are shown in Table D2 (b).

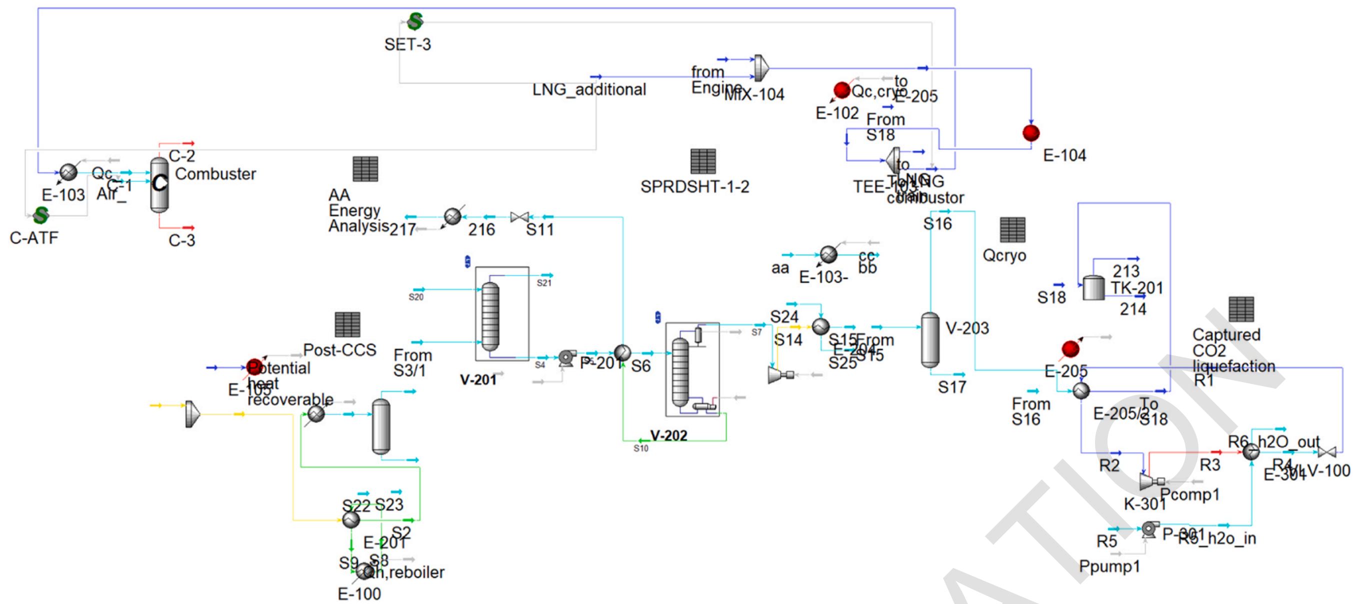

Figure D1. Aspen HYSYS process model of the amine-based post-combustion carbon capture (PostCCS) system, adapted from a validated steady-state model using blended MEA/MDEA solvent (Law et al., 2017a). The flowsheet includes key unit operations such as absorber, stripper, lean/rich heat exchanger, reboiler, condenser, and associated pumps. The absorber and stripper are modelled as packed columns with BXPLUS structured packing, and column dimensions are determined via hydraulic analysis to ensure operation below flooding limits

Table D2
(a) Key inputs for the amine-based post-combustion carbon capture (PostCCS) system, and (b) results obtained from the Aspen simulation and optimisation when the PostCCS system is sized to handle exhaust flow rate up to 12.14 kg/s and is operated at different exhaust feed flow rate

(a)

Input parameter	Normalised value	Sources
Solvent	MEA/MDEA blended amine Amine to water ratio: 4:6 MDEA to MEA ratio: 3:7 Lean amine condition: 30°C, 1 bar	Literature (Law et al., 2017a)
Seawater condition	25°C, 1 bar	Assumption
Production process & condition	1. CO_2 absorption by MEA/MDEA blended amine (30°C, 1 bar) 2. Amine regeneration at stripper (120°C, 2 bar) 3. CO_2 compression and liquefaction (−20°C, 20 bar)	Aspen optimised (Law et al., 2017a)
Liquid to gas ratio (by mass)	0.55 – 0.66	Aspen optimised to pass hydraulic test when the column is operated at different loads

(b)

Output parameter	Case 1	Case 2	Case 3	Case 4 (Maximum capacity)
Engine load (%)	25%	35%	50%	60%
Fuel Flow Rate@42.81MJ/kg (kg/h)	405.65	562.4	797.525	948
Exhaust Stack mass flow (kg/s)	6.16	7.87	10.43	12.14
CO_2 Mole/Wet Exhaust (%)	3.86%	4.10%	4.46%	4.53%
Required MEA/MDEA flow rate (kmol/h)	483	655	944	1117
CO_2 captured (kgCO_2/h)	1224	1630	2290	2711
reboiler duty (kW)	2500	2780	3268	3868
Heat recovery with exhaust WHR (kW)	423.9	575.9	831.8	968.5
Reboiler duty (with WHR) (MJ/kgCO_2)	6108	4867	3830	3852
Liquid to gas circulation rate (mass)	0.56	0.59	0.65	0.66

(continued on next column)

Table D2 (*continued*)

Pre-combustion carbon capture system

Hydrogen production from liquefied methane (LNG) is modelled via steam methane reforming (SMR) followed by water-gas shift (WGS) reactions. The reforming and shift reactors are represented using Gibbs reactors in Aspen HYSYS, where chemical equilibrium is determined through Gibbs free energy minimisation. The Peng–Robinson equation of state is employed as the thermodynamic property package to describe the gas-phase behaviour under varying operating conditions. The SMR unit converts methane and steam into syngas (H_2, CO, CO_2), which is subsequently processed through high-temperature water-gas shift (HTWGS) and low-temperature water-gas shift (LTWGS) reactors to maximise hydrogen production by converting CO into CO_2. Downstream of the shift reactors, a pressure swing adsorption (PSA) unit is implemented to separate high-purity hydrogen from CO_2 and residual gases. The captured CO_2 stream is further conditioned for storage, while the hydrogen-rich stream is utilised for onboard power generation via internal combustion engine (ICE) or gas turbine systems. The SMR model as shown in Fig. D3 is validated against experimental data reported in the literature (Law et al., 2023b), ensuring reliable prediction of hydrogen yield and CO_2 generation under relevant operating conditions. Table D4 shows the key inputs for the Aspen model of Pre-CCS system.

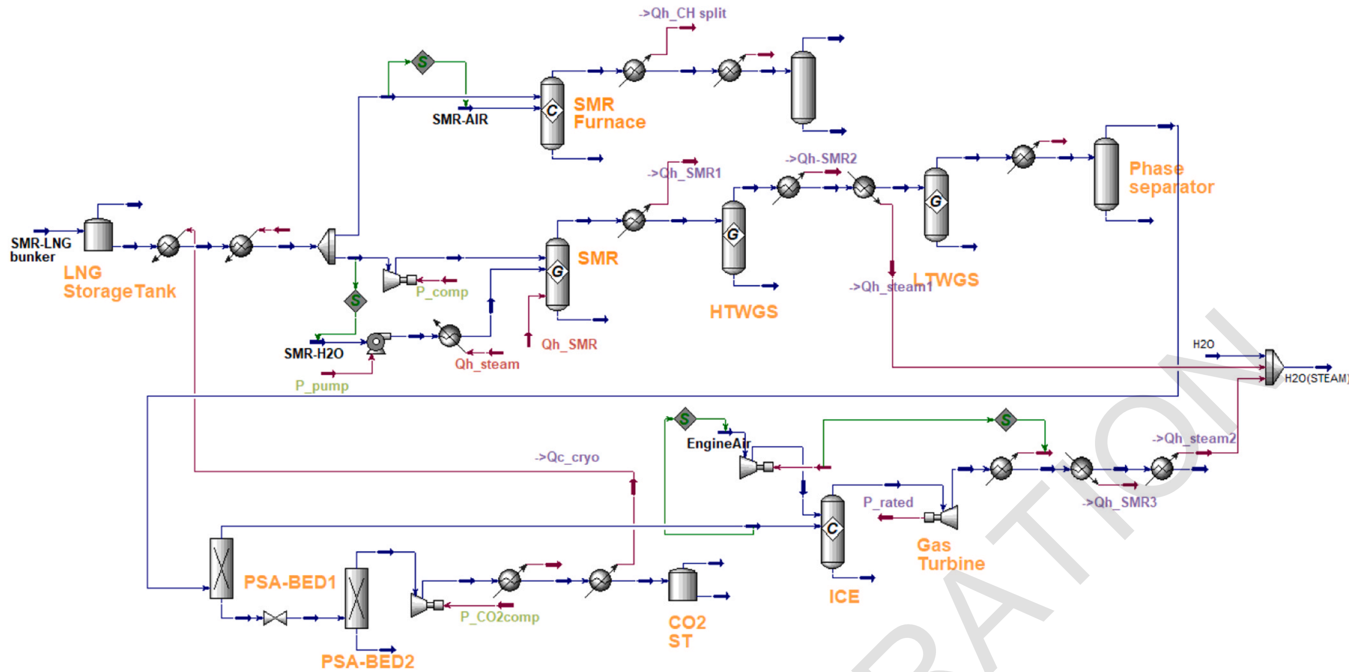

Figure D3. Aspen HYSYS process model of the pre-combustion carbon capture system (Pre-CCS) integrated with onboard hydrogen production via steam methane reforming (SMR). The flowsheet includes SMR and water-gas shift (HTWGS and LTWGS) reactors modelled as Gibbs reactors, followed by pressure swing adsorption (PSA) for hydrogen purification and CO_2 separation. The captured CO_2 is directed to storage, while the hydrogen-rich stream is utilised for onboard power generation. The model is validated against experimental data (Law et al., 2023b) and used for system sizing and integration within the shipboard decarbonisation framework

Table D4
Key inputs for the onboard hydrogen production unit pre-combustion carbon capture system (Pre-CCS). The process simulation and optimisation were conducted using Aspen HYSYS

Input parameter	Normalised value	Sources
Feedstock	LNG (assumed 100% methane), −162°C, 1 bar	Literature
Seawater condition	25°C, 1 bar	Assumption
Production process & condition	1. LNG vaporisation & compression (to 25 bar) 2. Steam methane reforming 3. HT water gas shift (500°C) 4. LT water gas shift (165°C) 5. H_2 purification and compression using PSA 6. CO_2 compression and liquefaction (−20°C, 20 bar)	Aspen simulated
Steam to fuel ratio	~3.163	Aspen optimised (Law et al., 2023b)
Furnace fuel source	Hydrogen product	Aspen optimised
Product	H_2 (also known as reformate), CO_2	Aspen simulated

Funding

This research was funded by the National Research Foundation (NRF), Prime Minister's Office, Singapore, under its Campus for Research Excellence and Technological Enterprise (CREATE) programme.

Declaration of Competing Interest

The authors declare that they have no known competing financial interests or personal relationships that could have appeared to influence the work reported in this paper.

Acknowledgment

For the purpose of open access, the authors have applied a Creative Commons Attribution (CC BY) license to any Author Accepted Manuscript version arising from this submission.

Appendix A. Ship data pre-processing

Table A1
Aggregated operational and energy performance metrics derived from the cleaned dataset. The data columns are the derived parameters from the raw data. The reported variables represent parameters derived from the processed raw data. The average diesel generator power (P_DG_Total) is calculated as the combined output of DG1, DG2, and DG3. Total distance is estimated from the cumulative distance travelled based on measured speed over ground. Fuel consumption (HFO and MDO) is

determined using fuel system status indicators (ON/OFF) together with mass flow meter measurements. Total CO_2 emissions are calculated by applying fuel-specific emission factors to the corresponding fuel consumption

Year	Month	Average of P_DG_Total (kW)	Average of P_ME (kW)	Total Distance (nm)	Total HFO (kg)	Total MDO (kg)	Total emissions (kg)
2023	January	379.58	2590.45	4813.29	401112.34	105792.73	1588235.32
2023	February	312.82	133.82	707.35	15013.04	102680.09	375942.98
2023	March	203.60	0.00	0.01	0.00	72827.76	233485.79
2023	April	271.68	493.30	1273.67	0.00	186147.01	596787.32
2023	May	420.18	4040.43	6920.99	475737.98	205572.08	2140512.17
2023	June	454.04	1942.48	3649.92	319888.48	269.06	996995.35
2023	July	417.05	4357.23	8064.16	677310.29	1.39	2109148.68
2023	August	341.05	833.28	3418.24	200446.02	33103.86	730319.89
2023	September	443.27	4212.49	7128.42	558179.43	41985.00	1872774.65
2023	October	464.16	1167.27	2473.33	233634.76	0.00	727538.65
2023	November	481.17	2792.56	5799.81	468028.38	0.00	1457440.37
2023	December	437.04	3745.13	6873.77	602452.86	0.00	1876038.20
2024	January	378.33	3695.49	6023.38	9630.27	317670.74	1048441.07
2024	February	336.82	764.43	1336.71	58350.76	94072.40	483300.39
2024	March	399.93	3024.04	5635.67	431888.03	60501.83	1538868.18
2024	April	440.43	2927.63	6271.23	367064.03	108752.55	1491698.07
2024	May	397.45	2196.54	5084.20	123859.20	239636.02	1153970.63
2024	June	433.97	2088.23	3962.11	241094.98	103355.73	1082128.24
2024	July	421.84	1987.42	4652.63	227936.42	111037.53	1065780.31
2024	August	453.23	4002.61	6172.96	562209.96	60090.74	1943372.74
2024	September	454.97	4202.23	6452.73	578241.88	65201.13	2009680.06
2024	October	392.29	2838.01	5536.57	368684.36	91143.92	1440290.50
2024	November	369.48	4438.71	6131.75	0.00	571666.34	1832762.29
2024	December	386.14	812.52	1881.75	0.00	136040.23	436144.98

Appendix B

Table B1
Emissions factors for various marine fuel pathways, extracted from preliminary study published in (Law et al., 2021)

Pathways	WtT (gCO2eq/MJ)	$C_{f,CO2}$ (gCO2eq/g fuel)	$C_{f,CH4}$ (gCH4/g fuel)	$C_{f,N2O}$ (gN2O/g fuel)	C_{slip} (as % of fuel mass)
HFO	13.5	3.114	0	0.00018	0
LNG	18.5	2.750	0	0.00011	3.1
Blue H2	132.0	0	0	0	0
Blue NH3	121.0	0	0	0	0
Blue MEOH	31.3	1.375	0	0	0
Blue E	27.8	0	0	0	0
Blue E-H2 (FC)	132.0	0	0	0	0
Blue E-NH3 (FC)	121.0	0	0	0	0
Blue E-MEOH	31.3	1.375	0	0	0
Solar E	19.17	0	0	0	0
Solar E-H2 (FC)	31.82	0	0	0	0
Solar E-NH3 (FC)	37.63	0	0	0	0
Solar E-MEOH	37.90	0	0	0	0

Table B2
Description and well-to-tank emissions factors of various biofuels pathways with the emission factors: biomass cultivation (e_{ec}), processing and production methods (e_p) and transportation (e_{td}) taken from EU Directive 2018/2001 (European Union, 2018). The summation of e_{ec}, e_p and e_{td} gives GHG_{WTT}

Pathways	Pathway Description	e_{ec}	e_p	e_{td}	GHG_{WTT}
Bio-ethanol 1	Ethanol, sugar beet ethanol (no biogas from slop, natural gas as process fuel in conventional boiler)	9.6	26.3	2.3	38.2
Bio-ethanol 2	Ethanol, sugar beet ethanol (with biogas from slop, natural gas as process fuel in conventional boiler)	9.6	13.6	2.3	25.5
Bio-ethanol 3	Ethanol, sugar beet ethanol (no biogas from slop, natural gas as process fuel in CHP plant)	9.6	18.5	2.3	30.4
Bio-ethanol 4	Ethanol, sugar beet ethanol (with biogas from slop, natural gas as process fuel in CHP plant)	9.6	10.6	2.3	22.5
Bio-ethanol 5	Ethanol, sugar beet ethanol (no biogas from slop, lignite as process fuel in CHP plant)	9.6	38.3	2.3	50.2
Bio-ethanol 6	Ethanol, sugar beet ethanol (with biogas from slop, lignite as process fuel in CHP plant)	9.6	22	2.3	33.9
Bio-ethanol 7	Ethanol, corn (maize) ethanol (natural gas as process fuel in conventional boiler)	25.5	29.1	2.2	56.8
Bio-ethanol 8	Ethanol, corn (maize) ethanol (natural gas as process fuel in CHP plant)	25.5	20.8	2.2	48.5
Bio-ethanol 9	Ethanol, corn (maize) ethanol (lignite as process fuel in CHP plant)	25.5	40.1	2.2	67.8
Bio-ethanol 10	Ethanol, corn (maize) ethanol (forest residues as process fuel in CHP plant)	25.5	2.6	2.2	30.3
Bio-ethanol 11	Ethanol, other cereals excluding maize ethanol (natural gas as process fuel in conventional boiler)	27	29.3	2.2	58.5
Bio-ethanol 12	Ethanol, other cereals excluding maize ethanol (natural gas as process fuel in CHP plant)	27	21.1	2.2	50.3
Bio-ethanol 13	Ethanol, other cereals excluding maize ethanol (lignite as process fuel in CHP plant)	27	42.5	2.2	71.7
Bio-ethanol 14	Ethanol, other cereals excluding maize ethanol (forest residues as process fuel in CHP plant)	27	2.2	2.2	31.4

(continued on next page)

Table B2 (*continued*)

Pathways	Pathway Description	e_{ec}	e_p	e_{td}	GHG_{WTT}
Bio-ethanol 15	Ethanol, sugar cane ethanol	17.1	1.8	9.7	28.6
Bio-ethanol 16	Ethanol, wheat straw ethanol	1.8	6.8	7.1	15.7
Bio-diesel 1	Bio-diesel, rape seed biodiesel	32	16.3	1.8	50.1
Bio-diesel 2	Bio-diesel, sunflower biodiesel	26.1	16.5	2.1	44.7
Bio-diesel 3	Bio-diesel, soybean biodiesel	21.2	16.9	8.9	47
Bio-diesel 4	Bio-diesel, palm oil biodiesel (open effluent pond)	26.2	42.6	6.9	75.7
Bio-diesel 5	Bio-diesel, palm oil biodiesel (process with methane capture at oil mill)	26.2	18.5	6.9	51.6
Bio-diesel 6	Bio-diesel, waste cooking oil biodiesel	0	13	1.9	14.9
Bio-diesel 7	Bio-diesel, animals fats from rendering biodiesel	0	19.1	1.7	20.8
Bio-diesel 8	Bio-diesel, waste wood Fischer-Tropsch diesel in free-standing plant	3.3	0.1	10.3	13.7
Bio-diesel 9	Bio-diesel, farmed wood Fischer-Tropsch diesel in free-standing plant	8.2	0.1	8.4	16.7
Bio-diesel 10	Bio-diesel, Fischer-Tropsch diesel from black-liquor gasification integrated with pulp mill	2.5	0	7.7	10.2
HVO 1	Hydrotreated Vegetable Oil (HVO), from rape seed	33.4	15	1.7	50.1
HVO 2	Hydrotreated Vegetable Oil (HVO), from sunflower	26.9	14.7	2	43.6
HVO 3	Hydrotreated Vegetable Oil (HVO), from soybean	22.1	15.2	9.2	46.5
HVO 4	Hydrotreated Vegetable Oil (HVO), from palm oil (open effluent pond)	27.4	38.9	7	73.3
HVO 5	Hydrotreated Vegetable Oil (HVO), from palm oil (process with methane capture at oil mill)	27.4	13.6	7	48
HVO 6	Hydrotreated Oil, from waste cooking oil	0	14.3	1.7	16
HVO 7	Hydrotreated Oil, from animal fats from rendering	0	20.3	1.5	21.8
PVO 1	Pure vegetable oil from rape seed	33.4	5.2	1.4	40
PVO 2	Pure vegetable oil from sunflower	27.2	5.4	1.7	34.3
PVO 3	Pure vegetable oil from soybean	22.2	5.9	8.8	36.9
PVO 4	Pure vegetable oil from palm oil (open effluent pond)	27.1	31.6	6.7	65.4
PVO 5	Pure vegetable oil from palm oil (process with methane capture at oil mill)	27.1	23.4	6.7	57.2
PO 1	Pure oil from waste cooking oil	0	0.8	1.4	2.2
Bio-MeOH 1	Bio-methanol, waste wood methanol in free-standing plant	3.1	0	10.4	13.5
Bio-MeOH 2	Bio-methanol, farmed wood methanol in free-standing plant	7.6	0	8.6	16.2
Bio-MeOH 3	Bio-methanol, methanol from black-liquor gasification integrated with pulp mill	2.5	0	7.9	10.4

Appendix C

Table C1
Energy and cost factors for selected marine fuel pathways, extracted from preliminary study published in (Law et al., 2021)

Pathways	E_{WTT} factor (MJ/MJ fuel)	$C_{TTW,Fuel}$ factor ($/MJ fuel)	$C_{TTW,EC}$ factor ($/kW)	$C_{TTW,Storage}$ factor ($/kJ)
HFO	0.0200	1.31E−02 (Ship and Bunker, 2025)[1]	1000	3.01E−05
LNG	0.0310	1.61E−02 (Ship and Bunker, 2025)[1]	1000	1.20E−04
Blue H2	0.4208	2.50E−02 (GEP, 2023)	1000	2.41E−04
Blue NH3	0.8300	2.80E−02 (Burgess et al., 2024)	1000	7.52E−05
Blue MEOH	0.8160	1.71E−02 (Procurement tactics, 2025)[3]	1000	4.01E−05
Blue E	0.8000	3.58E−02 (SP Group, 2025)[3]	500	3.71E−01
Blue E-H2 (FC)	1.4000	6.08E−02[3]	11,500	2.41E−04
Blue E-NH3 (FC)	1.7700	6.38E−02[3]	11,500	7.52E−05
Blue E-MEOH	1.7760	5.29E−02[3]	1000	4.01E−05
Biodiesel 1	0.0200	2.67E−02 (Procurement Resource, 2025)[4]	1000	3.01E−05
Biodiesel 2	0.0200	2.67E−02 (Procurement Resource, 2025)[4]	1000	3.01E−05
Solar E	0.0000	1.22E−02 (Jowett, 2024)[5]	500	3.71E−01
Solar E-H2 (FC)	0.6600	4.17E−02 (IEA, 2020)[6]	11,500	2.41E−04
Solar E-NH3 (FC)	0.9630	4.37E−02 (IRENE and Association, 2022)[7]	11,500	7.52E−05
Solar E-MEOH	0.9770	6.56E−02 (International Renewable Energy Agency; Methanol Institute, 2021)[8]	1000	4.01E−05

Note: 1. The bunker price for VLSFO was reported to be $550/MT (Integr8fuels, 2025; Ship and Bunker, 2025) and bunker price for LNG was reported to be around $800/MT at the Port of Rotterdam in Jan 2025 (Ship and Bunker, 2025), 2. Fossil-based methanol price equal to $340/metric tons (Procurement tactics, 2025); 3. The electricity supply for extra high tension (EHT) contracted supplies is 12.90 cents/kW (SP Group, 2025) hence the fuel cost for blue-E pathways were revised accordingly; 4. The price of biodiesel is largely influenced by region and regional feedstock prices, it is reported to range between $500 to more than $2000/MT (Procurement Resource, 2025), an intermediate value of $1000/MT was used.; 5. the average levelized cost of solar electricity is reported equal to $0.044/kWh by International Renewable Energy Agency (IRENE) (Jowett, 2024); 6. The average levelized cost for hydrogen produced with low carbon electricity is reported to range between $3.2 to $7.7/kg, an intermediate value of $5/kg is used (IEA, 2020); 7. The levelized cost for renewable ammonia is reported to range between $720-$1400/MT and is projected to reduce to $310–610/MT in 2050, an intermediate value of $900/MT is used (IRENE and Association, 2022). 8. The levelized cost for renewable methanol is reported to range between $800-$1600/MT and is projected to reduce to $250–630/MT in 2050, an intermediate value of $1000/MT is used (International Renewable Energy Agency; Methanol Institute, 2021).

Data availability

Data will be made available on request.

References

(IRENE), I.R.E.A., Association, A.E., 2022. Innovation outlook: renewable ammonia. Int. Renew. Energy Agency Abu Dhabi Ammon. Energy Assoc. Brooklyn.

ABS, "Advisory on Gas and Other Low Flashpoint Fuels," 2019. [Online]. Available: https://ww2.eagle.org/content/dam/eagle/advisories-and-debriefs/gas-and-low-flashpoint-fuels-advisory.pdf. [Accessed 24 September 2025].

Alkhaledi, A.N., Sampath, S., Pilidis, P., 2021. A hydrogen fuelled LH2 tanker ship design. Ships Offshore Struct. 19 (9), 1555–1564. https://doi.org/10.1080/17445302.2021.1935626.

Arachchige, U., Rasenthiran, K., Liyanage, M.P.P., 2019. Modelling Of CO 2 Capture Using Aspen Plus For Coal Fired Power Plant,". Int. J. Sci. Technol. Res. 8 (7), 316–318.

Arian, I.M., Putra, G.H., Akbar, T.A., 2018. Hazard identification of methanol fuel system on ship. Marit. Saf. Int. Conf.

Awoyomi, A., Patchigolla, Anthony, E.J., 2019. Process and Economic Evaluation of an Onboard Capture System for LNG-Fueled CO2 Carriers (p.). Ind. & Eng. Chem. Res. 59 (15). https://doi.org/10.1021/acs.iecr.9b04659 (p.).

Ayachi, F., Law, L.C., Mastorakos, E., Romagnoli, A., 2025. Comparative techno-economic analysis of integrated process designs combining LNG cold utilization and carbon capture. J. Clean. Prod. 524, 146274. https://doi.org/10.1016/j.jclepro.2025.146274.

Azemati, N., Zeraatgar, H., Zeraatgar, S., 2025. "Predicting and optimising ship fuel consumption using data-driven models and a proposed igwo algorithm for speed adjustment,". Pol. Marit. Res. 4 128, 40–58. https://doi.org/10.2478/pomr-2025-0049.

Bayraktar, M., Hazar, C., Yuksel, O., 2024. "Statistical analysis of the LNG-fueled marine vessels based on ship types and specifications,". Conf. Glob. Marit. Congr. 2024.

Bureau Veritas, 2023. Feasibility Study and Design Installing Carbon Capture and Storage Units on Existing Ships. Bur. Veritas Mar. Offshore Fr. (June).

Burgess, J., Garg, V., Gorman, M., 2024. Far East Asia leads global blue ammonia price gains in April. S&P Glob. https://www.spglobal.com/commodity-insights/en/news-research/latest-news/energy-transition/052124-far-east-asia-leads-global-blue-ammonia-price-gains-in-april.

Carbon Dioxide Properties, "CO2 Tables Web," Carbon Dioxide Properties, [Online]. Available: https://www.carbon-dioxide-properties.com/CO2TablesWeb.aspx. [Accessed 22 March 2025].

Dahlke-Wallat, F., Hoyer, K., Isidorović, L., Martens, S., Reinach, N., Friedhoff, B., Bačkalov, I., 2024. Ammonia Bunker Vessel: Ship Design for Energy Transition (Amsterdam, the Netherlands). Proceedings of 15th International Marine Design Conference (IMDC-2024).

DMA, "Chapter II-2 A: Fire protection, fire detection," 1 May 2007. [Online]. Available: https://www.dma.dk/Media/637743812057277254/D-II-2A-01052007.pdf. [Accessed 24 September 2025].

DNV, "DNV Awards AiP for HD Hyundai's Onboard Carbon Capture and Storage System Retrofit Design," DNV, 18 September 2024. [Online]. Available: https://www.dnv.com/news/dnv-awards-aip-for-hd-hyundais-onboard-carbon-capture-and-storagesystem-retrofit-design/. [Accessed 27 April 2025].

Du, Y., Gao, T., Rochelle, G.T., Bhown, A.S., 2021. Zero- and negative-emissions fossil-fired power plants using CO2 capture by conventional aqueous amines. Int. J. Greenh. Gas. Control. 111, 103473. https://doi.org/10.1016/j.ijggc.2021.103473.

EUR-Lex, "Directive 2009/31/EC of the European Parliament and of the Council of 23 April 2009 on the geological storage of carbon dioxide and amending Council Directive 85/337/EEC," 23 April 2009. [Online]. Available: https://eur-lex.europa.eu/legal-content/EN/TXT/?uri=CELEX%3A32009L0031. [Accessed 29 Sept 2024].

European Maritime Safety Agency (EMSA), "Study investigating the safety of hydrogen as fuel on ships," 10 July 2024a. [Online]. Available: https://emsa.europa.eu/publications/item/5263-mapping-safety-risks-for-hydrogen-fuelled-ships-study-investigating-the-safety-of-hydrogen-as-fuel-on-ships.html. [Accessed 14 April 2025].

European Maritime Safety Agency (EMSA), "Study investigating the safety of ammonia as fuel on ships," 10 July 2024b. [Online]. Available: https://emsa.europa.eu/publications/item/5264-study-investigating-the-safety-of-ammonia-as-fuel-on-ships.html. [Accessed 14 April 2025].

European Parliament and the Council of The European Union, 2023. Regulation (EU) 2023/1805 of the european parliament and of the council on the use of renewable and low-carbon fuels in maritime transport, and amending Directive 2009/16/EC. Off. J. Eur. Union. Eur. 13 September.

European Union, "Directive (EU) 2018/2001 of the European Parliament and of the Council on the promotion of the use of energy from renewable sources," 11 December 2018. [Online]. Available: https://eur-lex.europa.eu/legal-content/EN/TXT/PDF/?uri=CELEX:32018L2001.

Fan, H., 2021. IMO type C tank and FGSS solution for a retrofitted 10,000 TEU LNG-fuelled container ship (Singapore). C. -LNG Solut. Pte. Ltd. https://doi.org/10.13140/RG.2.2.24463.92321 (Singapore).

Fan, H., Xu, X., Abdussamie, N., Chen, P.S.-L., Harris, A., 2024. Comparative study of LNG, liquid hydrogen, and liquid ammonia post-release evaporation and dispersion during bunkering. Int. J. Hydrog. Energy 65, 526–539. https://doi.org/10.1016/j.ijhydene.2024.04.039.

Feenstra, M., Monteiro, J., Akker, J.T.V.D., Abu-Zahra, M.R., Gilling, E., Goetheer, E., 2019. Ship-based carbon capture onboard of diesel or LNG-fuelled ships. Int. J. Greenh. Gas. Control. 85, 1–10. https://doi.org/10.1016/j.ijggc.2019.03.008.

gCaptain, "World's Largest LNG-Fueled Ship Set for Delivery," gCaptain, 15 December 2017. [Online]. Available: https://gcaptain.com/worlds-largest-lng-fueled-ship-set-for-delivery/. [Accessed 20 March 2025].

GCMD; Stena Bulk; OGC, 2024. Project REMARCCABLE a case study for onboard carbon capture on the MR tanker stena impero. Oil Gas. Clim. Initiat.

GEP, "Outlook for Green abd Blue Hydrogen Market," 12 Jan 2023. [Online]. Available: https://www.gep.com/blog/strategy/Green-and-blue-hydrogen-current-levelized-cost-of-production-and-outlook. [Accessed 24 Feb 2025].

Geus-Moussault, S. d, Seubers, H., Linskens, H., Coraddu, A., Pruyn, J., 2024. Operational data for sea margin calculations in early ship design,". Proceedings of 15th International Marine Design Conference (IMDC-2024) https://doi.org/10.59490/imdc.2024.882.

Habibic, A., 2025. MAN ES checks off new milestone as full-scale ammonia engine runs at 100% load, 30 Jan Offshore Energy. https://www.offshore-energy.biz/man-es-checks-off-new-milestone-as-full-scale-ammonia-engine-runs-at-100-load/, 30 Jan.

M. Hand, "Alternative fuelled vessels – current numbers and forecasts," Seatrade Maritime News, 7 Sept 2022. [Online]. Available: c https://www.seatrade-maritime.com/alternative-fuels/alternative-fuelled-vessels-current-numbers-and-forecasts. [Accessed 25 Feb 2025].

Hansson, J., Klugman, S., Lönnqvist, T., Elginoz, N., Granacher, J., Hasselberg, P., Hedman, F., Efraimsson, N., Johnsson, S., Poulikidou, S., Safarian, S., Tjus, K., 2024. Biodiesel from Bark and Black Liquor—A Techno-Economic, Social, and Environmental Assessment. Energies 17 (1), 99. https://doi.org/10.3390/en17010099.

He, P., Jin, J.G., Pan, W., Chen, J., 2024. Route, speed, and bunkering optimization for lng-fueled tramp ship with alternative bunkering ports. Ocean. Eng. no 305 (3), 117957. https://doi.org/10.1016/j.oceaneng.2024.117957.

IEA, 2019. Hydrogen production costs using natural gas in selected regions, 2018. IEA [Online]. Available: https://www.iea.org/data-and-statistics/charts/hydrogen-production-costs-using-natural-gas-in-selected-regions-2018-2.

IEA, "Global average levelised cost of hydrogen production by energy source and technology, 2019 and 2050," 24 Sept 2020. [Online]. Available: https://www.iea.org/data-and-statistics/charts/global-average-levelised-cost-of-hydrogen-production-by-energy-source-and-technology-2019-and-2050. [Accessed 24 Feb 2025].

IMO,Resolution mepc.354(78) 2022 guidelines on the operational carbon intensity rating of ships (CII RATING GUIDELINES, G4)," 10 June 2022. [Online]. Available: https://wwwcdn.imo.org/localresources/en/KnowledgeCentre/IndexofIMOResolutions/MEPCDocuments/MEPC.354(78).pdf. [Accessed 11 November 2024].

IMO, 2023b. Revised GHG reduction strategy for global shipping adopted. IMO. https://www.imo.org/en/MediaCentre/PressBriefings/pages/Revised-GHG-reduction-strategy-for-global-shipping-adopted-.aspx.

IMO, 2023a. Marine Environment Protection Committee (MEPC 80), 3-7 July 2023. IMO. https://www.imo.org/en/MediaCentre/MeetingSummaries/Pages/MEPC-80.aspx.

IMO, "Resolution MEPC.376(80) Guidelines on Life Cycle GHG Intensity Gof Marine Fuels (LCA Guidelines)," 7 July 2023c. [Online]. Available: https://wwwcdn.imo.org/localresources/en/KnowledgeCentre/IndexofIMOResolutions/MEPCDocuments/MEPC.376(80).pdf. [Accessed 29 November 2023].

IMO, "IMO Data Collection System (DCS)," [Online]. Available: https://www.imo.org/en/OurWork/Environment/Pages/Data-Collection-System.aspx. [Accessed 8 January 2025].

Integr8fuels, "World Bunker Prices," Jan 2025. [Online]. Available: https://integr8fuels.com/world-bunker-prices/. [Accessed 24 Feb 2025].

International Energy Agency (IEA), 2017. IEAGHG Technical Report 2017-02 Techno-Economic Evaluation of SMR Based Standalone (Merchant) Hydrogen Plant with CCS. IEA Environ. Proj. Ltd. Chelten. UK.

International Maritime Organisation (IMO), 2025. International Code of Safety for Ship Using Gases or Other Low-flashpoint Fuels (IGF Code). IMO. https://www.imo.org/en/ourwork/safety/pages/igf-code.aspx.

International Renewable Energy Agency; Methanol Institute, 2021. Innovation Outlook: Renewable Methanol. Int. Renew. Energy Agency Abu Dhabi.

P. Jowett, "Global average solar LCOE stood at $0.044/kWh in 2023, says IRENA," PV Magazine, 27 September 2024. [Online]. Available: https://www.pv-magazine.com/2024/09/27/global-average-solar-lcoe-stood-at-0-044-kwh-in-2023-says-irena/. [Accessed 24 Feb 2025].

Juliana Monteiro, Research Scientist at TNO, "CO2ASTS – carbon capture, storage and transfer in shipping," CO2ASTS Project, Germany-Netherlands, 2020.

Kanchiralla, F.M., Brynolf, S., Olsson, T., Ellis, J., Hansson, J., Grahn, M., 2023. How do variations in ship operation impact the techno-economic feasibility and environmental performance of fossil-free fuels? A life cycle study (no). Appl. Energy 350. https://doi.org/10.1016/j.apenergy.2023.121773.

Kim, D., Jang, S., Lee, J.-i, Rhee, S.H., Kwon, H., Jeong, H., 2026. Ship operational data driven fuel efficiency assessment for shaft generator using input convex neural network. Energy Rep. 15, 108993. https://doi.org/10.1016/j.egyr.2025.108993.

Korberg, A., Brynolf, S., Grahn, M., Skov, I., 2021. Techno-economic assessment of advanced fuels and propulsion systems in future fossil-free ships. Renew. Sustain. Energy Rev. 142. https://doi.org/10.1016/j.rser.2021.110861.

Law, L.C., Azudin, N., Shukor, S.R.A., 2017b. "Optimization and economic analysis of amine-based acid gas capture unit using monoethanolamine/methyl diethanolamine,". Springe Link. 20, pages451–461.

Law, L.C., Azudin, N., Syamsul Rizal Abdul Shukor, 2017a. Optimization of Operational Parameter and Economic Analysis of Amine Based Acid Gas Capture Unit. Chem. Eng. Trans. 56, 73–78. https://doi.org/10.3303/CET1756013.

Law, L.C., Foscoli, B., Mastorakos, E., Evans, S., 2021. A Comparison of Alternative Fuels for Shipping in Terms of Lifecycle Energy and Cost. Energies 14 (24). https://doi.org/10.3390/en14248502 (p.).

Law, L.C., Gkantonas, S., Mengoni, A., Mastorakos, E., 2024. "Onboard pre-combustion carbon capture with combined-cycle gas turbine power plant architectures for LNG-fuelled ship propulsion,". Appl. Therm. Eng. 248 (Part B), 123294. https://doi.org/10.1016/j.applthermaleng.2024.123294.

Law, L.C., Mastorakos, E., Evans, S., 2022. Estimates of the Decarbonization Potential of Alternative Fuels for Shipping as a Function of Vessel Type, Cargo, and Voyage. Energies 15 (7468). https://doi.org/10.3390/en15207468.

Law, L.C., Mastorakos, E., Othman, M.R., Trakakis, A., 2023b. "A thermodynamics model for the assessment and optimisation of onboard natural gas reforming and carbon capture,". Emiss. Control. Sci. Technol. 10, 52–69. https://doi.org/10.1007/s40825-023-00234-z.

Law, L.C., Othman, M.R., Mastorakos, E., 2023a. "Numerical analyses on performance of low carbon containership,". Energy Rep. 9, 3440–3457. https://doi.org/10.1016/j.egyr.2023.02.035.

Lee, S., Yoo, S., Park, H., Ahn, J., Chang, D., 2021. Novel methodology for EEDI calculation considering onboard carbon capture and storage system. Int. J. Greenh. Gas. Control. 105. https://doi.org/10.1016/j.ijggc.2020.103241 (no.).

Lin, M., 2022. Conversion-ready' boxships pay well for shipowners in low-carbon future: study. S&P Glob. https://www.spglobal.com/commodity-insights/en/news-research/latest-news/shipping/092922-conversion-ready-boxships-pay-well-for-shipowners-in-low-carbon-future-study 29 Sep.

Lloyd's Register, 2025. IMO Marine Environment Protection Committee (MEPC 83): Summary Report. Lloyd'S. Regist.

Lloyd's Register, "LR-RU-012 Classification of Ships using Gases or other Low-flashpoint Fuels," LR, 1 July 2025. [Online]. Available: https://www.lr.org/en/knowledge/lloyds-register-rules/rules-and-regulations-for-ships-using-gases-or-low-flashpoint-fuels. [Accessed 24 September 2025].

Long, N.V.D., Lee, D.Y., Kwag, C., Lee, Y.M., Lee, S.W., Hessel, V., Lee, M., 2021. Improvement of marine carbon capture onboard diesel fueled ships. Chem. Eng. Process. - Process. Intensif. 168. https://doi.org/10.1016/j.cep.2021.108535.

Luo, X., Wang, M., 2017. Study of solvent-based carbon capture for cargo ships through process modelling and simulation (no). Appl. Energy 195, 402–413. https://doi.org/10.1016/j.apenergy.2017.03.027.

Majer, S., (DBFZ), K.O., (AKB), F.K., (EBA), S.S., 2016. BIOSURF Fuelling Biomethane: D5.3 | Calculation of GHG emission caused by biomethane. Eur. Union. 'S. Horiz. 2020 Res. Innov. Program.

MAN Energy Solutions, 2024. MITSUI Performs World-First Hydrogen Test. MAN Energy Solut. https://www.man-es.com/company/press-releases/press-details/2024/03/07/mitsui-performs-world-first-hydrogen-test#:~:text=MITSUI%20Performs%20World%2DFirst%20Hydrogen,that%20uses%20hydrogen%20as%20fuel.%E2%80%9D 7 March.

Martinić-Cezar, S., Jurić, Z., Assani, N., Lalić, B., 2024. Optimization of Fuel Consumption by Controlling the Load Distribution between Engines in an LNG Ship Electric Propulsion Plant. Energies . 17, 3718. https://doi.org/10.3390/en17153718.

Mehedi, T.H., Gemechu, E., Kumar, A., 2022. "Life cycle greenhouse gas emissions and energy footprints of utility-scale solar eenrgy systems,". Appl. Energy 314, 118918. https://doi.org/10.1016/j.apenergy.2022.118918.

MEPC, "ANNEX 3, Resolution MEPC. 278 (70)," 28 October 2016. [Online]. Available: https://wwwcdn.imo.org/localresources/en/OurWork/Environment/Documents/278%2870%29.pdf. [Accessed 8 January 2025].

National Renewable Energy Laboratory, "Life Cycle Greenhouse Gas Emissions from Solar Photovoltaics," 2012. [Online]. Available: https://www.nrel.gov/docs/fy13osti/56487.pdf. [Accessed 24 April 2025].

Nugent, D., Sovacool, B.K., 2014. "Assessing the lifecycle greenhouse gas emissions from solar PV and wind energy: A critical meta-survey,". Energy Policy 65, 229–244. https://doi.org/10.1016/j.enpol.2013.10.048.

OGCI, Stena Bulk, and TNO, "Is Carbon Capture on Ship Feasible," Oil and Gas Climate Initiative, November, 2021.

Oh, J., Kim, D., Roussanaly, S., Anantharaman, R., Lim, y, 2023. Optimal capacity design of amine-based onboard CO2 capture systems. Prepr. Submitt. LAPSE (Living Arch. Process. Syst. Eng. https://doi.org/10.13140/RG.2.2.33147.69922.

Oh, J., Kim, D., Roussanaly, S., Lim, Y., 2024. Greenhouse gas emissions of shipping with onboard carbon capture under the FuelEU Maritime regulation: A well-to-wake evaluation of different propulsion scenarios (no). Chem. Eng. J. 498. https://doi.org/10.1016/j.cej.2024.155407.

Øi, L.E., 2007. "Aspen HYSYS Simulation of CO 2 Removal by Amine Absorption from a Gas Based Power Plant,". SIMS2007 Conference, Gøteborg.

N.H. Prevljak, "ClassNK okays 'world's first' onboard CCS installation on Neopanamax," Offshore Energy, 21 March 2024. [Online]. Available: https://www.offshore-energy.biz/classnk-okays-worlds-first-onboard-ccs-installation-on-neopanamax/. [Accessed 25 Feb 2025].

Procurement Resource, "Biodiesel Price TRend and Forecast," 2025. [Online]. Available: https://www.procurementresource.com/resource-center/biodiesel-price-trends. [Accessed 24 Feb 2025].

Procurement tactics, 2025. Methanol Prices – Historical Graph. Procure. Tactics. In: https://procurementtactics.com/methanol-prices/.

Raucci, C., Calleya, J., Fuente, S.S.D.L., Pawling, R., 2015. Hydrogen Onboard Ship: A First Analysis of Key Parameters and Implications. Int. Conf. Shipp. Chang. Clim. 2015 2015.

Ricardo, 2024. Review of Existing Practices on Marine Fuel Sustainability Aspects/Certification and Third-Party Verification Issues. Ricardo Ref. ED18601 Oxfs. UK.

Riviera News, "MOL and Mitsui win AiP for ammonia-powered bulk carrier," RIviera, 27 Jan 2023. [Online]. Available: https://www.rivieramm.com/news-content-hub/news-content-hub/mol-and-mitsui-win-aip-for-ammonia-powered-bulk-carrier-74739. [Accessed 20 March 2025].

Ros, J.A., Skylogianni, E., Doedée, V., Akker, J.T. v d, Vredeveldt, A.W., Linders, M.J., Goetheer, E.L., Monteiro, J.G.M.-S., 2022. Advancements in ship-based carbon capture technology on board of LNG-fuelled ships (no.). Int. J. Greenh. Gas. Control. 114. https://doi.org/10.1016/j.ijggc.2021.103575 (no.).

Ruan, Z., Huang, L., Li, D., Ma, R., Wang, K., Zhang, R., Zhao, H., Wu, J., Li, X., 2025. "A novel dual-stage grey-box stacking method for significantly improving the extrapolation performance of ship fuel consumption prediction models,". Energy 318, 134927. https://doi.org/10.1016/j.energy.2025.134927.

R.M. Sari and K. Kolmetz, "GENERAL PROCESS PLANT COST ESTIMATING, Kolmetz Handbook of Process Equipment Design," June 2014. [Online]. Available: https://www.researchgate.net/publication/336591395_GENERAL_PROCESS_PLANT_COST_ESTIMATING_Kolmetz_Handbook_of_Process_Equipment_Design. [Accessed 12 April 2025].

SEA-LNG, 2019. Comparison of Alternative Marine Fuels. DNVGL. https://sea-lng.org/wp-content/uploads/2020/04/SEA-LNG_Alternative_fuels_narrative_V22.pdf.

Ship & Bunker, 2025. Rotterdam Bunker Prices. Ship Bunker. https://shipandbunker.com/prices/emea/nwe/nl-rtm-rotterdam#VLSFO, 24 Feb.

SP Group, "Electricity Tariff Revision for the Period 1 January to 31 March 2025," 30 December 2024. [Online]. Available: https://www.spgroup.com.sg/about-us/media-resources/news-and-media-releases/Electricity-Tariff-Revision-for-the-Period-1-January-to-31-March-2025. [Accessed 24 Feb 2025].

Stec, M., Tatarczuk, A., Iluk, T., Szul, M., 2021. Reducing the energy efficiency design index for ships through a post-combustion carbon capture process. Int. J. Greenh. Gas. Control. 108. https://doi.org/10.1016/j.ijggc.2021.103333 (no.).

Tuswan, T., Sari, D.P., Muttaqie, T., Prabowo, A.R., Soetardjo, M., Murwantono, T.T.P., Utina, R., Yuniati, Y., 2023. Representative application of LNG-fuelled ships: a critical overview on potential GHG emission reductions and economic benefits. N. Int. J. Nav. Archit. Ocean. Eng. Res. Dev. 74. https://doi.org/10.21278/brod74104 (no.).

U.S. Department of Energy, 2025. Alternative Fuels Data Center. Off. Energy Effic. Renew. Energy. https://afdc.energy.gov/fuels/biodiesel-benefits#:~:text=The%20flashpoint%20for%20biodiesel%20is,Use%20Guide%20(Sixth%20Edition)%20.

Wärtsilä, "Onboard carbon capture and storage: pioneering solution for ships," Wärtsilä, 27 June 2022. [Online]. Available: https://www.wartsila.com/marine/products/exhaust-treatment/carbon-capture-and-storage?gad_source=1&gad_campaignid=22743706223&gbraid=0AAAAABRKeTW7uZe10xpuhe6FTdJFetMpi&gclid=Cj0KCQjwrojHBhDdARIsAJdEJ_cSUUtYrkm44TaZ86SiF0mPFYbtSQsWa5vLINaR1M1JHIdFv1IJSOUaA. [Accessed 5 October 2025].

World Economic Forum, "These emerging economies are poised to lead shipping's net-zero transition," World Economic Forum, 18 August 2022. [Online]. Available: https://www.weforum.org/agenda/2022/08/maritime-shipping-decarbonization-emerging-economies/. [Accessed 8 January 2024].

Zervos, Z., Themelis, N., 2021. A Comparison Study of Ship Fuel Oil Consumption Based on Theoretical and Data-Driven Models. Conference: 15th Annual Conference of Hellenic Institute of Marine Technology.At: Athens, Greece.

Zhang, M., Tsoulakos, N., Kujala, P., Hirdaris, S., 2024a. A deep learning method for the prediction of ship fuel consumption in real operational conditions. Eng. Appl. Artif. Intell. 130 (2024), 107425. https://doi.org/10.1016/j.engappai.2023.107425.